Scaling for interfacial tensions near critical endpoints

Shun-yong Zinn and Michael E. Fisher
Institute for Physical Science and Technology, University of Maryland, College Park, Maryland 20742, USA
(Received 9 August 2004; published 6 January 2005)

Parametric scaling representations are obtained and studied for the asymptotic behavior of interfacial tensions in the *full* neighborhood of a fluid (or Ising-type) critical endpoint, i.e., as a function *both* of temperature *and* of density/order parameter *or* chemical potential/ordering field. Accurate *nonclassical critical exponents* and reliable estimates for the *universal amplitude ratios* are included naturally on the basis of the "extended de Gennes–Fisher" local-functional theory. Serious defects in previous scaling treatments are rectified and complete wetting behavior is represented; however, quantitatively small, but unphysical residual nonanalyticities on the wetting side of the critical isotherm are smoothed out "manually." Comparisons with the limited available observations are presented elsewhere but the theory invites new, searching experiments and simulations, e.g., for the vapor-liquid interfacial tension on the two sides of the critical endpoint isotherm for which an amplitude ratio -3.25 ± 0.05 is predicted.

DOI: 10.1103/PhysRevE.71.011601 PACS number(s): 68.05.−n, 64.60.Fr, 64.70.Fx, 05.70.Jk

I. INTRODUCTION AND SCALING THEORY

Consider, for concreteness, a binary liquid mixture consisting of two species, A and B. For a full thermodynamic description, one needs three field variables, say (T,h,g) [1,2]. The ordering field h is conjugate to the order parameter, M. For fluids, the order parameter may (in leading order) be taken as the number density $\Delta\rho=\rho-\rho_0(T,g)$ measured relative to a coexistence value $\rho_0(T,g)$. Alternatively, M could be a composition variable such as mole fraction difference, a volume fraction difference, and so forth. For the nonordering field g, one may take the pressure, or the chemical potential of one species, either A or B, etc.

Figure 1(a) illustrates a typical phase diagram in the three-dimensional field space [2]. At any point on the surface labeled $\tilde{h}=0$, the system exhibits phase separation into two coexisting phases, β and γ, rich in A and B, respectively. We will adopt the convention that the γ phase has the higher (mass) density and hence sits at the bottom of a container when a gravitational field is present: see the inset in Fig. 1(a). By increasing temperature while keeping $\tilde{h}\equiv h-h_0(T,g)=0$, the state point will reach the line λ which is a locus of critical points, $T_c(g)$. Further temperature increase results in mixing of the β and γ phases into a single phase, say $\beta\gamma$. On the other hand, decreasing g at fixed $T<T_c(g)$ on the $\tilde{h}=0$ surface leads to a triple-point line, τ, at which appears a new, noncritical or "spectator" phase α which represents the common vapor of the liquid phases β, γ, and $\beta\gamma$: see the inset in Fig. 1(a). A first-order transition, between the vapor and the liquid phases, occurs across the vapor-pressure surface labeled σ which meets the $\tilde{h}=0$ surface at the triple line. The critical line, λ, and the triple point line, τ, terminate at a point $(T_e,0,g_e)$: that is the "critical endpoint."

Recent field-theoretic renormalization group theory has confirmed explicitly that the critical behavior at a critical endpoint is the same as on the critical locus [3,4]. Nevertheless, further, new bulk thermodynamic singularities do appear at a critical endpoint [5–7].

Beyond the bulk, however, there are singularities in *interfacial* or *surface tensions* when, in the presence of the vapor α, the two phases β and γ merge into the homogeneous phase $\beta\gamma$, or vice versa [5,6]. In Fig. 1(a) one may follow the triple line and its smooth extension on the σ surface, beyond the critical endpoint, or, in Fig. 1(b), simply trace the line $g_\sigma(T)$. The "critical surface tension" between the coexisting phases vanishes below the critical endpoint temperature $T_c=T_e$, as

$$\Sigma_{\beta|\gamma}(T)\approx K|t|^{\mu},\quad t\equiv(T-T_e)/T_e\to 0-,\quad (\tilde{h}=0), \tag{1.1}$$

where, via standard scaling relations [1,5,8–10], the critical exponent is given by $\mu=2-\alpha-\nu$ so that $\mu\simeq 1.26$ for typical, three-dimensional fluids. The amplitude K has dimensions of energy per unit area where, here and below, we adhere to the notation set out in the Appendix of Ref. [8]. The "noncritical tensions," $\Sigma_{\alpha|\beta\gamma}$ and $\Sigma_{\alpha|\beta}$, should behave [1,5], after subtraction of a suitable, nonsingular common background, $\Sigma_0(T)$, as

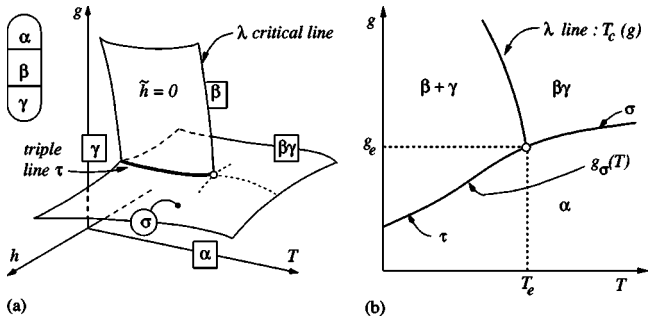

FIG. 1. (a) Phase diagram of a binary liquid mixture in the three-dimensional field space (T,h,g): see text for details. (b) Section of the phase diagram (a) containing the plane $\tilde{h}=0$. The critical endpoint,(T_e,g_e), is where the critical line λ terminates at the first-order transition line $g_\sigma(T)$.

$$\Delta\Sigma_{\alpha|\beta\gamma} \approx K^+|t|^\mu, \quad t \to 0+, \quad (\tilde{h}=0), \tag{1.2}$$

$$\Delta\Sigma_{\alpha|\beta} \approx K^-|t|^\mu, \quad t \to 0-, \quad (\tilde{h}=0-), \tag{1.3}$$

which relations serve to define the amplitudes K^+ and K^-. Beneath T_c the γ phase coexists with the α and β phases and, in a sealed container, it sits below the β phase owing to its presumed heavier density. Now consider, hypothetically, bringing into contact the two phases α and γ, near $\beta\gamma$ criticality; this produces a new interface. The corresponding noncritical surface tension $\Sigma_{\alpha|\gamma}$ can be obtained from Antonow's rule [1] which states

$$\Sigma_{\alpha|\gamma}(T) = \Sigma_{\alpha|\beta}(T) + \Sigma_{\beta|\gamma}(T). \tag{1.4}$$

This relation can be derived by supposing that the three phases α, β, and γ can coexist and meet with nonzero contact angles, and then by letting the contact angle between the interfaces $\alpha|\beta$ and $\beta|\gamma$ go to zero [1]. (It should be recalled, however, that Antonow's rule typically fails at lower temperatures, specifically below a wetting temperature T_W.)

Using the classical van der Waals or Cahn-Hilliard theory [11] and a model free energy of the Landau-expansion type, Widom [12] has studied various properties of the noncritical interfaces, such as that between α and β, near the critical endpoint. Later, nonclassical critical exponents were embodied into the local free energy expression via postulated scaling forms [10]. However, the original theory of Widom and Ramos-Gómez [10] led to an unexpected type of correction in the surface tension, namely a $|t|^\gamma$ term: this is *more singular* than the nonanalytic leading term $|t|^\mu$ whenever the spatial dimensionality, d, exceeds $3-\eta$ [5,6] which cannot be considered acceptable.

Fisher and Upton [5] pointed out that, near the critical endpoint, the amplitude ratios

$$P \equiv (K^+ + K^-)/K, \quad Q \equiv K^+/K^-, \tag{1.5}$$

should be *universal*. They reported mean-field calculations [5,6,10] yielding

$$P = -\tfrac{1}{2}(\sqrt{2}-1) = -0.20710\ldots, \quad Q = -\sqrt{2}, \tag{1.6}$$

which should be valid for $d>4$. However, to obtain more realistic values for $d=3$, Fisher and Upton [5,6] presented preliminary calculations using an extended de Gennes–Fisher (EdGF) local functional theory [6] for fluid interfaces combined with a simple "interpolated linear model" for the equation of state (as described in Ref. [9]). This approach provided the significantly different estimates

$$P \simeq 0.1_2, \quad Q \simeq -0.83. \tag{1.7}$$

More recently, the EdGF theory has also been applied to critical adsorption problems [13].

Our aim here, apart from estimating these universal ratios more precisely, is to calculate the noncritical surface tension in *nonzero ordering field*, i.e., $\Delta\Sigma_{\alpha|\beta\gamma}$, $\Delta\Sigma_{\alpha|\beta}$, and $\Delta\Sigma_{\alpha|\gamma}$ as a function of *t and h* (or the order parameter, M), on the σ surface in the *full* vicinity of a critical endpoint. This is a basic problem of interfacial thermodynamics first broached experimentally in pioneering work by Nagarajan, Webb, and Widom [14]. In fact, there is just a single function of two variables, $\Delta\Sigma(t,h)$, that is to be sought once a suitable background $\Sigma_0(t,h)$ is subtracted from the total surface tension, say $\Sigma_{\alpha|\bullet}(t,h)$. Furthermore, in the first instance our main concern must be with the singular, critical behavior which we may confidently expect to be described in scaling form so that $\Delta\Sigma/|t|^\mu$ is related universally (for $d<4$) to the scaled combination $M/|t|^\beta$ or, equivalently, to $\tilde{h}/|t|^\Delta$, where, in standard notation, $\Delta=\beta+\gamma=\beta\delta$.

Three decades after the development of renormalization group theory one might expect this problem to be susceptible to such an approach. Unfortunately, however, the still remaining difficulties, both technical and conceptual, are profound despite the progress reported, for example, in the review articles by Abraham, by Diehl, and by Jasnow in Ref. [49] and subsequent developments (some of which are referenced in further detail below). Accordingly we report here on calculations based on *local functional theories* going back historically to van der Waals' analysis of the critical surface tension $\Sigma_{\beta|\gamma}(T)$. Specifically, we pick up and develop the proposals of Fisher and Upton [6] who advanced, in particular, the EdGF theory which can consistently embody the correct nonclassical critical point exponents, especially $\eta>0$.

Such theories rely on the availability of an accurate description of the *bulk* thermodynamic properties. To that end we will make heavy use of the *parametric formulation* of scaling theory in the neighborhood of a bulk critical point as extended to represent the true correlation length, $\xi_\infty(T,h)$, and so provide a basis for calculating interfacial tensions via local functional theories [6,8,9]. For completeness and ease of reference we recall the basic parametric expressions here. As standard, one first has

$$t = rk(\theta), \quad h = r^\Delta l(\theta), \quad M = r^\beta m(\theta), \tag{1.8}$$

where $k(\theta)$ is an even function of the "angular" variable θ with $k_0 \equiv k(0)=1$ and $k(\pm\theta_c)=0$ so that $\theta=\pm\theta_c$ corresponds to the critical isotherm, $T=T_c$, while $l(\theta)$ and $m(\theta)$ are odd, with $l(0)=m(0)=0$ and $l(\pm\theta_1)=0$ with $m(\theta_1)>0$ so that $\theta=\pm\theta_1$ describes the coexistence surface $\tilde{h}=0$ beneath T_c: see Fig. 2 of [9].

For general thermodynamic purposes, however, it proves more effective to avoid integrating the equation of state to obtain the free energy; accordingly [9], we opt to treat h [and $l(\theta)$] as derived from the singular part of the reduced Helmholtz free energy which may be written in scaling form as

$$\mathcal{A}_s(t,M) = r^{2-\alpha} n(\theta), \tag{1.9}$$

where, following [9], we can write

$$n(\theta) = r^{-2+\alpha}\mathrm{sing}\left\{ \int_{M_R}^{M} h(M';T)\,dM' \right\}, \tag{1.10}$$

in which the operation sing$\{\bullet\}$ extracts only the leading singular part while $M_R<0$ is a fixed reference value: see also (2.1) below. One then finds that $l(\theta)$ is readily expressed in terms of $k(\theta)$ and $n(\theta)$: see Eq. (4.4) of [9].

The generalized local functional theories proposed in [6] also require the true correlation length, $\xi_\infty(T,h)$, which specifies the exponential decay of correlations (in the presumed *absence* of long-range power-law or van-der-Waals-type interactions). The corresponding scaling form can be written [9]

$$\xi_\infty^2/2\chi = r^{-\eta\nu} a_\infty(\theta), \tag{1.11}$$

where $\chi=(\partial M/\partial h)_T$ is the reduced compressibility (or susceptibility) while η and ν are the standard correlation critical exponents. It is worth stressing that an essential feature of the generalized local functional theories [6] is to provide in a consistent way for $\eta>0$ since this is vital for the accurate description of real and realistic model systems when $d<4$.

The local functional theories, if they are to yield computations for the *interfacial tension*, also require that $\mathcal{A}_s(M,T)$ and $\xi_\infty^2/2\chi$ are well defined *through* the two-phase region below T_c where $|M|$ is less than $M_0(T)\approx B|t|^\beta$, the order parameter at coexistence (or, in magnetic terms, the spontaneous magnetization). While this is most certainly questionable from a rigorous viewpoint, one may in practice construct *trigonometric forms* for $k(\theta)$, $m(\theta)$, $n(\theta)$, etc., which extrapolate smoothly (and, indeed, analytically) to $|\theta|>\theta_1$ and so through the two-phase region: see [6,8,9]. In such cases we take $k(\theta)$, $m(\theta)$, etc., as smooth periodic functions, of appropriate parity, in the interval $-\theta_0\leqslant\theta\leqslant\theta_0$ where θ_0 then corresponds to $h=M=0$ for $T<T_c$. On this framework an "extended sine model" has been built and fitted to reliable estimates of critical exponents and amplitude ratios for the $(d=3)$-dimensional Ising model [9]. The resulting scaling functions will be used here to study the interfacial tensions near a critical endpoint.

In the scaling region the singular part of the full interfacial tension can consequently be written parametrically as

$$\Delta\Sigma(t,h) = r^\mu s(\theta), \tag{1.12}$$

and our basic task is to calculate the angular surface tension function $s(\theta)$. Note that $\Delta\Sigma$ represents (i) $\Delta\Sigma_{\alpha|\beta\gamma}$ when $|\theta|<\theta_c$, (ii) $\Delta\Sigma_{\alpha|\beta}$ when $\theta_c<\theta\leqslant\theta_1$, and (iii) $\Delta\Sigma_{\alpha|\gamma}$ when $-\theta_1\leqslant\theta\leqslant-\theta_c$, in accordance with Fig. 1 and the notation explained above. Once $s(\theta)$ is determined, the surface tension can also be written in the standard scaling form

$$\Delta\Sigma \approx K|t|^\mu S_\pm(\bar{D}h/|t|^\Delta), \tag{1.13}$$

where the universal scaling function $S_\pm(x)$ can be readily calculated. (Note that, as customary, the subscripts + and − stand for $t\geqslant 0$ and $t\leqslant 0$, respectively.) The amplitudes K and $\bar{D}$ here are the nonuniversal metric factors needed for normalization and to make $S_\pm(x)$ and the argument x, dimensionless. In the notation of [8] we take $\bar{D}=C^+/B$ and $x=\tilde{h}$, which provided a convenient normalized variable in the analysis of Ref. [9].

Experimentally, as mentioned, Nagarajan, Webb, and Widom (NWW) [14] were the first to test theoretical predictions for the universal surface-tension scaling functions off the $\tilde{h}=0$ axis in their studies of mixtures of isobutyric acid and water. For the same mixture, Howland, Wang and Knobler [15] measured the critical surface tension $\Sigma_{\beta|\gamma}$ and Greer [16] measured densities on the coexistence curve. The two latter experiments can be used to provide a consistency check and calibration of the NWW data [17]. Other mixtures have also been examined. Quasi-binary mixtures of *n*-octadecane and *n*-nonadecane in ethane have been studied by Pegg *et al.* [18] to measure the surface tensions through and near both the upper and the lower critical endpoints. The surface tension of the water and 2,5-lutidine system at and off the critical composition has been measured by Amara *et al.* [19]. For a similar mixture of water and 2,6-lutidine, Mainzer-Althof and Woermann determined the values of P and Q experimentally [20]. Interfacial tensions of the critical mixture of 2-butoxyethanol and water have been measured by Ataiyan and Woermann [21]. The applications of the present theory to these various data will be presented elsewhere [22].

The rest of this article proceeds as follows. In Sec. II, we review briefly the classical theory of interfaces. The construction of more general local free energy functionals is taken up in Sec. III. Following Fisher and Upton [5,6] we work out the details of the extended de Gennes–Fisher (EdGF) ansatz and obtain formulae for the equilibrium order parameter profile and the surface tension. The hypothesis that the noncritical vapor phase α can be replaced by a wall with a surface field h_1 [5,6] is introduced in Sec. IV. In the scaling limit $h_1/|t|^{\Delta_1}\to-\infty$ (where Δ_1 is the appropriate *surface* critical exponent), there appear terms in the total wall tension that diverge although remaining analytic in t. After subtracting these divergent terms, we can express the finite singular part of the surface tension near a critical endpoint explicitly in parametric scaling form. In Sec. V these expressions are evaluated numerically for $d=3$. However, an unphysical although quite small *cusp* is uncovered in the basic scaling function $s(\theta)$ in (1.12). Its origin is discussed and found to reside in a fairly subtle deficiency of the EdGF scheme. By using an interpolation scheme, the cusp can be smoothed out leading to acceptable approximations for the universal scaling functions $S_\pm(x)$ in (1.13). On this basis various concrete numerical results are presented in Sec. VI for the surface tensions in the vicinity of a critical endpoint. Section VI contains some brief concluding remarks.

II. LOCAL FUNCTIONAL THEORIES FOR FLUID INTERFACES

A. The auxiliary free energy function

Let us consider various free energies that will be needed in discussing the local-functional theory of fluid interfaces in a general way. Let $A(M,T)$ be the true equilibrium Helmholtz free energy density that preserves the appropriate convexity properties in M and T [23]. The free energy density $A(M,T)=A_{\text{total}}(M,T)/V$ can be obtained by integrating the equation of state,

$$A(M,T) = \int_{M_R}^{M} h(M')dM' + A(M_R,T), \tag{2.1}$$

using a fixed reference value $M_R\neq 0$: such a choice of reference value guarantees no singularity across $t=0$ in $A(M_R,T)$.

In order to keep track of dimensions, we take M as the density difference $(\rho-\rho_c)$ from now on.

Now let $A^\dagger(M,T)$ be the Helmholtz free energy density in the one-phase region and its presumed analytic continuation into the multiphase region [6,8,9]. The typical van der Waals loop, which does not respect the convexity, should appear in the multiphase region of $A^\dagger(M,T)$. The Maxwell construction applied to $A^\dagger(M,T)$ repairs the convexity (although this is, of course, *ad hoc*). Evidently, $A(M,T)=A^\dagger(M,T)$ outside the multiphase region while $A^\dagger(M,T)\geqslant A(M,T)$ inside. The excess free energy $A^\dagger(M,T)-A(M,T)$ which is then always nonnegative, serves in the local functional theories, to determine the structures of the interfaces between the coexisting phases [24].

The conjugate free energy density $F(h_\infty,T)=F_{\text{total}}(h_\infty,T)/V$, where the subscript ∞ denotes a bulk equilibrium quantity, may be obtained from $A(M,T)$ via the Legendre transform,

$$F(h_\infty;T) \equiv \min_M[A(M,T)-h_\infty M], \tag{2.2}$$

$$=A(M_\infty,T)-h_\infty M_\infty, \tag{2.3}$$

where $M_\infty=M(T,h_\infty)$ is the bulk equilibrium value of the order parameter.

The interfacial tension that we aim to calculate is the excess free energy of a system in equilibrium created by one or more interfaces. All local functional theories for interfaces introduce an auxiliary free energy $W[M(z);T,h_\infty]$ that resembles the excess free energy: $W(M)$ is always nonnegative and vanishes only when the profile, $M(z)$, takes an equilibrium value of the order parameter corresponding to one of the coexisting phases (M_α for the α phase, M_β for β, etc.). Since the equilibrium values of the order parameter M_α, M_β, etc., are specified both by T and h_∞, the dependence of the auxiliary free energy on T and h_∞ must not be overlooked.

Thus the auxiliary free energy function $W(M;T,h_\infty)$ needed in a local functional theory can be defined by [5,6]

$$W(M;T,h_\infty) \equiv A^\dagger(M,T)-h_\infty M-F(h_\infty,T), \tag{2.4}$$

$$=A^\dagger(M,T)-A^\dagger(M_\infty,T)-h_\infty(M-M_\infty), \tag{2.5}$$

where we have used $A^\dagger(M_\infty)=A(M_\infty)$. Since $A^\dagger(M)$ represents the analytic continuation of $A(M)$, we may also use (2.1) to write

$$W(M;T,h_\infty)=\int_{M_\infty}^{M} h(M',T)dM'-h_\infty(M-M_\infty), \tag{2.6}$$

because the equation of state must then equally have an analytic continuation: notice that $A(M_R,T)$ cancels out. From this one immediately finds that $W(M_\infty;T,h_\infty)=0$ and $(\partial W/\partial M)_{M=M_\infty}=0$. Starting from $A^\dagger(M,T)\geqslant A(M,T)$ and using (2.2) and (2.4) one obtains

$$W(M;T,h_\infty)\geqslant A(M,T)-h_\infty M-\min_M[A(M,T)-h_\infty M]\geqslant 0. \tag{2.7}$$

Thus, $W(M;T,h_\infty)$ vanishes at the equilibrium values of M for all T and h_∞ and its leading term in the expansion about M_∞ is quadratic in $(M-M_\infty)$. Otherwise, W takes only positive values.

B. van der Waals theory

It is helpful to review briefly the van der Waals theory of interfaces which is a Landau-type classical theory [1,11,25]. Assuming the existence of the local free energy $W[M(z);T,h_\infty]$ that can be expanded in powers of M and $T-T_c$, the van der Waals theory takes the local excess free-energy density functional as a sum of two terms [1], namely,

$$\Delta f[M(z)]=W[M(z)]+\tfrac{1}{2}J_0\left(\frac{dM}{dz}\right)^2, \tag{2.8}$$

where J_0 $(=\xi^2/\chi)$ is a constant and z is the perpendicular distance from the interface presumed to be flat. The square-gradient term, $(dM/dz)^2$, accounts for spatial inhomogeneity in the simplest manner. The overall excess free energy is then given by a volume integral of $\Delta f(z)$. Translational invariance parallel to the interface enables one to factor out the area in the volume integral so that the free energy per unit area, or surface tension, can be written as [1]

$$\Sigma[M(z)]=\int dz\,\Delta f[M(z)]. \tag{2.9}$$

Functional minimization of $\Sigma[M]$ with respect to $M(z)$ yields a differential equation for the equilibrium order parameter profile $M(z)$. To supply boundary conditions let us consider, for example, a system containing two bulk equilibrium phases with $M=M_\beta$ (or $M_{-\infty}$) and M_γ (or $M_{+\infty}$) located at $z=-\infty$ and $+\infty$, respectively. For convenience, M_β and M_γ can be taken equal in magnitude but opposite in sign $(M_\gamma>0)$. Then, near criticality the equilibrium order parameter profile behaves like $M_\gamma\tanh(z/\xi)$ for the stated boundary conditions and the resulting surface tension is

$$\Sigma=\int_{M_\beta}^{M_\gamma} dM\sqrt{2J_0W(M)}. \tag{2.10}$$

With a suitable representation for $W[M]$, one can also study the critical and noncritical surface tensions [10,12], as well as the critical wetting transition [26]. However, this classical square-gradient theory *cannot* satisfactorily embody all the correct critical exponents. This is because the square-gradient term in (2.8), when the analysis is adapted to study the decay of correlations (rather than just the overall interfacial free energy), always implies the exponent value $\eta=0$ that is valid only for $d\geqslant 4$. Thus even upon using an equation of state that obeys scaling and embodies correct exponents (such as the extended sine model discussed in [9]), a square-gradient form for the local free-energy yields the classical value $\eta=0$ for the correlation function decay [27].

III. FISHER-UPTON THEORY FOR FLUID INTERFACES

In order to generalize the classical square-gradient theory, we start with the total free energy of the binary mixture written in the form

$$F_{\text{total}}(T,h_\infty,g) = \min_{M(\mathbf{r})} \mathcal{F}[M], \tag{3.1}$$

where $\mathcal{F}[M;T,h_\infty]$ is a sought-for local free energy functional. Assuming translational invariance along directions parallel to the interfaces, we may simply take $M(\mathbf{r})=M(z)$. The solution $M(z)$ that minimizes the functional $\mathcal{F}[M]$ is the equilibrium order parameter profile for the specified T, h_∞, and boundary conditions. We can suppose that $\mathcal{F}[M]$ has a homogeneous part describing the uniform bulk phases and an inhomogeneous part $\Delta\mathcal{F}$, so that

$$\mathcal{F}[M(z)] = F_{\text{bulk}}(T,h_\infty,g) + \Delta\mathcal{F}, \tag{3.2}$$

where $F_{\text{bulk}}(T,h_\infty,g)$ is the bulk free energy (and g is the third field: see Fig. 1). If there were no interfaces, we would have $\Delta\mathcal{F}=0$, and $F_{\text{total}}=F_{\text{bulk}}$. Following [6], we now consider a general local free energy functional of the form

$$\Delta\mathcal{F} = \int d\mathbf{r}\mathcal{A}(M,\dot{M};T,h_\infty,g), \tag{3.3}$$

where $\dot{M} \equiv dM/dz$. Without great loss of generality, we may write [6]

$$\mathcal{A}(M,\dot{M};T,h_\infty,g) = W(M)[1 + J(M)\mathcal{G}(\Lambda\dot{M})], \tag{3.4}$$

where J and Λ are to be functions of M and T. The function $\mathcal{G}(x)$ should be even since the sign of $\dot{M}$ cannot matter in the free energy. Now $\mathcal{A}$ should vanish when $\dot{M}=0$ so that $\Delta\mathcal{F}=0$; this implies $\mathcal{G}(0)=0$. To determine other properties of $\mathcal{G}(x)$ we must proceed further.

For semi-infinite cases where an external wall is located at $z=0$, the postulate (3.3) must be modified by adding a boundary term [28]

$$\frac{\Delta\mathcal{F}[M]}{A} = \int_0^\infty dz\, \mathcal{A}(M,\dot{M}) + f_1(M_1;h_1), \tag{3.5}$$

where A is the area of the interface. The surface field h_1 acts only at $z=0$ and is coupled to $M_1 \equiv M(z=0)$, the order parameter on the boundary.

Now let us minimize

$$\frac{\Delta\mathcal{F}[M(z)]}{A} = \int_0^\infty dz[\mathcal{A}(M,\dot{M}) + \delta(z)f_1(M)] \tag{3.6}$$

with respect to $M(z)$ where the boundary term has been absorbed into the integral. Then in the usual way, integrating by parts, one obtains

$$\frac{\delta\Delta\mathcal{F}[M(z)]}{A} = \int_0^\infty dz\left[\left\{\frac{\partial\mathcal{A}}{\partial M} - \frac{d}{dz}\left(\frac{\partial\mathcal{A}}{\partial\dot{M}}\right)\right\}\delta M + \delta(z)\left\{\frac{df_1}{dM} - \frac{\partial\mathcal{A}}{\partial\dot{M}}\right\}\delta M\right] + \left.\frac{\partial\mathcal{A}}{\partial\dot{M}}\delta M\right|_{z=\infty}, \tag{3.7}$$

and hence finds

$$\frac{\partial\mathcal{A}}{\partial M} - \frac{d}{dz}\left(\frac{\partial\mathcal{A}}{\partial\dot{M}}\right) = 0, \tag{3.8}$$

$$\left(\frac{\partial\mathcal{A}}{\partial\dot{M}}\right)_{z=0} - \frac{df_1}{dM_1} = 0, \quad \text{and} \quad \left.\frac{\partial\mathcal{A}}{\partial\dot{M}}\right|_{z=\infty} = 0. \tag{3.9}$$

However, since $\mathcal{A}(M,\dot{M})$ has no explicit z-dependence, we can integrate (3.8) to get the first-order differential equation

$$\mathcal{A}(M,\dot{M}) - \dot{M}\frac{\partial\mathcal{A}}{\partial\dot{M}} = \mathcal{C}, \tag{3.10}$$

in which $\mathcal{C}$ is a constant.

Now consider a fully infinite situation so that the lower limit in (3.5) becomes $-\infty$ and the surface term drops out. Functional minimization again yields (3.8), and thence (3.10), while the first (wall) condition in (3.9) becomes simply the bulk condition $(\partial\mathcal{A}/\partial\dot{M})_{z=-\infty}=0$.

In the semi-infinite situation, the form (3.4) leads to

$$W(M_1)J(M_1)\Lambda(M_1)\mathcal{G}'(\Lambda\dot{M})\big|_{z=0} = \frac{df_1}{dM_1}, \tag{3.11}$$

which is an equation determining M_1. Similarly, the two bulk conditions yield

$$\left.\frac{\partial\mathcal{A}}{\partial\dot{M}}\right|_{z=\pm\infty} = W(M_{\pm\infty})J(M_{\pm\infty})\Lambda(M_{\pm\infty})\mathcal{G}'(\Lambda\dot{M}_{\pm\infty}) = 0; \tag{3.12}$$

but since $W(M_{\pm\infty})=0$ these conditions should hold automatically provided that $J(M_{\pm\infty})$, $\Lambda(M_{\pm\infty})$, and $\mathcal{G}'(\Lambda\dot{M}_{\pm\infty})$ do not diverge. We will see below that these functions have nice behavior so that we may forget the bulk conditions.

Far away from the wall or the interfaces, in the infinite and semi-infinite cases, one should see only the bulk behavior of the system. Hence, it is natural to require

$$M(z) \to M_{\pm\infty}, \quad \dot{M}(z) \to 0, \quad \text{as } |z| \to \infty. \tag{3.13}$$

Because $\mathcal{A}(M_{\pm\infty},0)=0$ the constant $\mathcal{C}$ in the first integral (3.10) must thus vanish. Then using the postulate (3.4) one is led to

$$x \equiv \Lambda(M)\dot{M} = \frac{1 + J(M)\mathcal{G}(x)}{J(M)\mathcal{G}'(x)}, \tag{3.14}$$

which represents a differential equation for the equilibrium profile $M_{\text{eq}}(z)$.

In order to devise appropriate expressions for $\mathcal{A}(M,\dot{M})$ which generalize the earlier de Gennes–Fisher theory [29], applicable only at $T=T_c$, Fisher and Upton [6] introduced the following desirable physical features or desiderata:

A. The correct, non-classical critical exponents should be embodied, both in $d=2$ and in $d=3$. Conversely, a reduction to van der Waals or Landau theory should be implied whenever the classical critical exponents are assumed.

B. Near the critical point, all thermodynamic functions should satisfy the scaling and analyticity requirements: in particular, singularities (or nonanalyticities) should appear only at bulk criticality, i.e., when $t=h=M_\infty=0$.

C. For the semi-infinite system, the critical-point decay of the profile should behave in accordance with scaling as [29,30]

$$M_c(z) \sim z^{-\beta/\nu}. \tag{3.15}$$

D. When two plates separated by a finite distance L are immersed in a critical system, the order parameter decay (3.15) should have a correction factor so that

$$M_c(z) \sim z^{-\beta/\nu}[1 + j_2(z/L)^{d^*} + \cdots], \quad L \to \infty, \tag{3.16}$$

where $d^* = (2-\alpha)/\nu$ and j_2 is some coefficient. This prediction of the de Gennes–Fisher theory [29] has been verified by several analyses including exact Ising model calculations for $d=2$ [5,6] and field-theoretic calculations in $\epsilon=4-d$ dimensions [31–33].

E. Away from criticality, the order parameter should always decay exponentially

$$\Delta M(z) \equiv M(z) - M_\infty \sim e^{-z/\xi}, \quad z \to \infty, \tag{3.17}$$

where, clearly, $\xi(T,h)$ denotes the *true* correlation length, ξ_∞, but for brevity we will neglect the subscript ∞. (Note again that we are assuming the absence of power-law forces or the likelihood that, if present, they do not enter explicitly into the asymptotic scaling functions.)

F. For a finite critical slab, in the same situation as **D**, the critical profile will exhibit a *minimum* for similar boundary conditions satisfying $M(z=0)$, $M(z=L)>0$, or a *zero* for opposing boundary conditions $M(z=0)>0$ and $M(z=L)<0$ [34]. It is expected that this profile, $M_c(z)$, behaves analytically near $z=z_0$ as

$$M_c(z) = k_1(z-z_0)^{\lambda_1}[1 + k_2(z-z_0)^{\lambda_2} + \cdots], \tag{3.18}$$

where **F(i)** $\lambda_1=0$ for the similar case, or $\lambda_1=1$ for the opposing case; **F(ii)** for the further exponents, one should have $\lambda_2=2$, $\lambda_4=4$, etc.

G. Away from criticality a square-gradient expansion in the local free energy functional is expected to be correct and so should be reproduced by a satisfactory theory.

H. To describe adsorption on a wall at $z=0$, the theory should be consistent with the thermodynamic relation

$$\Gamma \equiv \int_0^\infty \Delta M(z)dz = -\left(\frac{\partial \Sigma}{\partial h}\right)_T, \tag{3.19}$$

where Σ is the wall (or surface) free energy.

I. The order parameter profile $M(z;T,h,g;L)$ should be analytic in all noncritical regions. (Compare with **B** above.)

The starting point of the Fisher-Upton theory is the de Gennes–Fisher (dGF) ansatz [29] for $T=T_c$ which in the general expression (3.4) is given by [5,6],

$$J = \text{const}, \quad \Lambda(M) = \xi(M)/M, \quad \mathcal{G}(x) = |x|^{2-\tilde{\eta}},$$
$$\text{with} \qquad \tilde{\eta} = 2\eta/(d^* + \eta). \tag{3.20}$$

This form satisfies **A**–**D** and **F(i)**. However, the dGF theory applies only *at* criticality. The extension proposed by Fisher and Upton (EdGF) uses $\chi(M,T)=(\partial M/\partial h)_T$ and postulates

$$J = 1, \quad \Lambda(M;T,h_\infty,g) = \sqrt{\xi^2(M,T)/2\chi(M,T)W(M;T,h_\infty)}. \tag{3.21}$$

In order to satisfy **E**, one finds that the condition

$$\hat{\mathcal{G}}(1) = 1 \qquad \text{with} \qquad \hat{\mathcal{G}}(x) \equiv x\mathcal{G}'(x) - \mathcal{G}(x), \tag{3.22}$$

must be satisfied. Also, in order to satisfy **F**, $\mathcal{G}(x)$ should behave as

$$\mathcal{G}(x) = G_0 + G_\infty|x|^{2-\tilde{\eta}}[1 + l_1x^{-\tau} + l_2x^{-2\tau} + \cdots],$$
$$\text{with} \qquad \tau = 2\beta/(\beta+\nu). \tag{3.23}$$

Finally, for small $x \to 0$ the validity of a gradient expansion, **G**, can be seen to require [5,6]

$$\mathcal{G}(x) = x^2 + G_2x^4 + G_4x^6 + \cdots. \tag{3.24}$$

Using the EdGF postulate (3.21) and the condition (3.22), the solution of the general profile equation (3.14) reduces to $x=\pm 1$, or

$$\dot{M} = \pm 1/\Lambda(M), \tag{3.25}$$

where the signs $\pm$ must be chosen appropriately. Hereafter, we take the $+$ sign, for an increasing profile as $z \to +\infty$. The wall free energy then follows from (3.5) as

$$\Sigma = \Delta\mathcal{F}[M_{\text{eq}}(z)]/A = [1 + \mathcal{G}(1)]\int_0^\infty dz\, W(M) + f_1(M_1), \tag{3.26}$$

where (3.3), (3.21), and (3.25), and $\mathcal{G}(-x)=\mathcal{G}(x)$ have been used. Using (3.25) once again, one can rewrite the semi-infinite integral as

$$\Sigma = [1 + \mathcal{G}(1)]\int_{M_1}^{M_\infty} dM\, W(M)\Lambda(M) + f_1(M_1). \tag{3.27}$$

Now the thermodynamic consistency condition, **H**, leads to [6]

$$1 + \mathcal{G}(1) = 2 \qquad \text{or} \qquad \mathcal{G}(1) = 1. \tag{3.28}$$

It is remarkable that both the profile and the wall or interfacial free energy, $\Sigma(T,h)$, do not depend on the details of $\mathcal{G}(x)$ [6]. However, one must note that the EdGF ansatz fails to satisfy **I** in certain situations [6].

In order to repair this last problem, a generalized de Gennes–Fisher ansatz (GdGF) was devised [6]. It satisfies all

of the desiderata **A**–**I**. However, in contrast to the EdGF theory, the profile equation, the surface tension formulae, etc., now depend on $\mathcal{G}(x)$ explicitly. In order to obtain quantitative results, one must devise a representation for $\mathcal{G}(x)$ that reproduces (3.23) and an analogue of (3.24). One can indeed achieve this; but the resulting calculations become considerably more complicated than those for the EdGF theory. Accordingly we have explored numerically only the EdGF formulation.

It must be recognized, however, that both EdGF and GdGF theories ignore capillary-wave fluctuations of a free interface, which are important for $d \leqslant 3$ [5,6]. Also, as indicated above, the analytic continuations of $W(M)$, $\xi^2(M)/2\chi(M)$, etc., into the multi-phase region have no known meaning in the strict sense of rigorous statistical mechanics. However, we expect that both theories will produce reasonably reliable results when fitted to exact $d=2$ and $d=4$ results and good estimates for various $d=3$ parameters, since they embody many correct physical features.

Indeed, Upton's $\epsilon=4-d$ expansion results for the universal amplitude ratio $Q=K^+/K^-$ [35] demonstrate this point quite well. Using the field-theoretic approach to surface critical phenomena, he obtained the exact ϵ-expansion $Q=-\sqrt{2}+1.521\,257\epsilon+\mathcal{O}(\epsilon^2)$. Then, using the EdGF theory and the linear parametric model (which is known to be exact to order ϵ^2 [36,37]), he found $Q=-\sqrt{2}+1.522\,96_2\epsilon+\mathcal{O}(\epsilon^2)$. The coefficients of ϵ differ by only 0.1%.

IV. EdGF EXPRESSIONS FOR SURFACE TENSION NEAR A CRITICAL ENDPOINT

We now discuss in more explicit detail the application of the EdGF theory sketched above to the vicinity of a critical endpoint. Allowing for a boundary term, which will be discussed further below, (3.27) can be written as

$$\Sigma(T,h,g) = 2\int_{M_1}^{M_\infty} dM\sqrt{W(M)\xi^2(M)/2\chi(M)} + f_1(M_1), \tag{4.1}$$

where the arguments h_∞ and T are understood and (3.21) and (3.28) have been used.

A. Scaling forms

To embody the appropriate nonclassical critical exponents and satisfy the desiderata **A** and **B** we should, clearly, adopt scaling forms for $W(M;T,h_\infty)$ and the combination $\xi^2(M,T)/\chi(M,T)$. As discussed, the required expressions must continue analytically (or, at least, sufficiently smoothly) into the two-phase region $|M|<M_0(T)$. We should also recall the necessity for including the further field g and the lambda line $T=T_c(g)$: see Fig. 1. Following [9], we thus introduce the dimensionless asymptotic scaling variables

$$\tilde{m} \equiv M/B|\tilde{t}\,|^\beta, \quad \tilde{h} \equiv [h-h_0(T,g)]/(B/C^+)|\tilde{t}\,|^{\beta+\gamma}, \tag{4.2}$$

where the reduced temperature deviation is now [5,6]

$$\tilde{t} = [T - T_c(g)]/T_e, \tag{4.3}$$

while, for convenience, the tilde on h now denotes the fully scaled field and, for brevity, the phase boundary term, $h_0(T,g)$, will usually be neglected below. As usual [8] $B=B(g)$ and $C^+=C^+(g)$ are, respectively, the critical amplitudes of the spontaneous order, $M_0(T,g)\approx B|t|^\beta$, and the susceptibility, $\chi_0^+(T,g)=(\partial M/\partial h)_{T>T_c}\approx C^+/t^\gamma$, on the $\tilde{h}=0$ surface above $T_c(g)$.

Then, following [5,6], we can write the scaling form

$$\xi^2(M,T,g)/2\chi(M,T,g) \approx |M|^{-\eta\nu/\beta} Z_\pm(\tilde{m}), \tag{4.4}$$

which is crucial in going beyond van der Waals or Landau square-gradient theory because it introduces the small but positive (for $d<4$) exponent η. As above, the subscripts $+$ and $-$ will always denote $\tilde{t}>0$ or <0, respectively. However, it must be realized here and below that the scaling functions Z_+ and Z_- and, likewise, others are, in fact, representations of a *single*, generally analytic scaling function continuing smoothly through $t \gtrless 0$. Thus, more explicitly, to ensure the analyticity of $\xi^2/2\chi$ across the surface $T=T_c(g)$ or $\tilde{t}=0$ (recall **B**) the scaling functions $Z_\pm$ must have large $\tilde{m}$ expansions of the form

$$Z_\pm(\tilde{m}) = Z_0^\infty\left[1 + \sum_{n=1}^{\infty} Z_n^\infty(\pm|\tilde{m}|^{-1/\beta})^n\right]. \tag{4.5}$$

When $T \to T_c(g)\pm$ the terms in the sum clearly generate only the integral powers $\tilde{t}^{\,n}$ as required by analyticity when $M \neq 0$.

The correct analyticity is most conveniently incorporated by using the parametric representations of the scaling functions recalled in Sec. I. The only new features required near a critical endpoint are the replacement of t by $\tilde{t}$, as defined in (4.3) and allowance for the (smooth) dependence of the nonuniversal factors $m_0 \equiv m(0)$ and $l_0 \equiv l(0)$ on the field g: see (1.8) and [38]. With this understanding the parametric forms (1.8)–(1.10) will be adopted. Then one can express the coefficients entering (4.5) as

$$Z_0^\infty = a_\infty(\theta_c)[m(\theta_c)]^{\eta\nu/\beta} \equiv a_{\infty c}(m_c)^{\eta\nu/\beta}, \tag{4.6}$$

$$Z_1^\infty = \frac{[m_c/B]^{1/\beta}}{k_c'}\left\{\frac{a_{\infty c}'}{a_{\infty c}} + \frac{\eta\nu}{\beta}\frac{m_c'}{m_c}\right\}, \tag{4.7}$$

$$Z_2^\infty = \frac{[m_c/B]^{2/\beta}}{2[k_c']^2}\left\{\frac{2(1+\eta\nu)}{\beta}\frac{a_{\infty c}'}{a_{\infty c}}\frac{m_c'}{m_c} + \frac{\eta\nu(2-\beta-\eta\nu)}{\beta^2}\left(\frac{m_c'}{m_c}\right)^2 + \frac{a_{\infty c}''}{a_{\infty c}} - \frac{a_{\infty c}'}{a_{\infty c}}\frac{k_c''}{k_c'} + \frac{\eta\nu}{\beta}\left(\frac{m_c'}{m_c}\frac{k_c''}{k_c'} - \frac{m_c''}{m_c}\right)\right\}, \tag{4.8}$$

where the prime denotes differentiation and for brevity we have used $a_{\infty c}' \equiv a_\infty'(\theta_c)$, etc., and so on.

The required scaling form for $W(M;T,h_\infty)$ must be somewhat more elaborate because of the additional dependence on h_∞: see the original definition (2.5). (Indeed, the result presented in [6] is somewhat misleading since the dependence on h_∞ was suppressed and the expressions given apply

only for $h_\infty = 0$.) Let us consider, first, the parametric representation for W following from (2.6) with the aid of (1.10). Note that specification of T and h_∞ implies, via (1.8), parametric coordinates r_∞ and θ_∞ (for the corresponding bulk phase) while the variation of M at constant T and h_∞ can be described by coordinates r and θ. Thus from (2.6) and (1.8) we obtain

$$W(r,\theta;r_\infty,\theta_\infty) \approx r^{2-\alpha} n(\theta) - r_\infty^{2-\alpha} n(\theta_\infty) - r_\infty^{\Delta} l(\theta_\infty)[r^\beta m(\theta) - r_\infty^\beta m(\theta_\infty)]. \quad (4.9)$$

When $t \neq 0$, the relation $t = rk(\theta) = r_\infty k(\theta_\infty)$ leads to the desired form

$$W(M;T,h_\infty) \approx r^{2-\alpha} w(\theta;\theta_\infty), \quad (4.10)$$

where, with $h_\infty = r_\infty^\Delta l(\theta_\infty)$ and (1.8) for M, we have

$$w(\theta;\theta_\infty) = n(\theta) - l(\theta_\infty) m(\theta) |k(\theta)/k(\theta_\infty)|^\Delta - [n(\theta_\infty) - l(\theta_\infty) m(\theta_\infty)] |k(\theta)/k(\theta_\infty)|^{2-\alpha}, \quad (4.11)$$

while the singular part of the Helmholtz free energy *extended into the two-phase region*, as discussed above, is given by (1.9) [39].

When $T = T_c$ we have $\theta = \theta_\infty = \theta_c$ and $w(\theta;\theta_\infty)$ simplifies to yield

$$w_c \equiv w(\theta_c;\theta_c) = \beta m_c l_c/(2-\alpha), \quad (4.12)$$

$$w_c' \equiv \left(\frac{dw}{d\theta}\right)_{\theta=\theta_\infty=\theta_c} = \frac{\beta m_c l_c' - (1-\beta) l_c m_c'}{(1-\alpha)}. \quad (4.13)$$

Consequently $w(\theta;\theta_\infty)$ is continuous and smooth through $T = T_c(g)$ (or $\theta = \theta_\infty = \theta_c$). However, the presence of the powers of Δ and $(2-\alpha)$ in (4.11) shows that the curvature $(d^2w/d\theta^2)$ is *not* continuous through $T = T_c(g)$. Nevertheless, this lack of analyticity of $w(\theta;\theta_\infty)$ is not, of itself, expected to lead to corresponding nonanalytic behavior in surface free energies, etc., since the underlying bulk free energies and correlation lengths do vary analytically.

Now we can express W in the alternative scaling form

$$W(M;T,h_\infty) \approx |M|^{\delta+1} Y_\pm(\tilde{m};\tilde{h}_\infty) \quad (4.14)$$

where, with $A^\infty(\tilde{h}_\infty) = -n(\theta_\infty)/|k(\theta_\infty)|^{2-\alpha}$, we have

$$Y_\pm(\tilde{m};\tilde{h}_\infty) = A^\infty(\tilde{h}_\infty)|B\tilde{m}|^{-\delta-1} - h_\infty[M - M_\infty(T,h_\infty)]|M|^{-\delta-1} + Y_0^\infty\left[1 + \sum_{n=1}^{\infty} Y_n^\infty (\pm|\tilde{m}|^{-1/\beta})^n\right]. \quad (4.15)$$

[This reduces to the Fisher-Upton expressions when $h_\infty \to 0$ for $\tilde{t} > 0$ and $\tilde{t} < 0$ although Eq. (7) of [6], should be corrected by changing $(\pm|y|)^{-n/\beta}$ to read $(\pm|y|^{-1/\beta})^n$.] On rearranging for $|\tilde{m}| \to \infty$ we have

$$Y_\pm(\tilde{m};\tilde{h}_\infty) = Y_0^\infty[1 \pm Y_1^\infty|\tilde{m}|^{-1/\beta} - \mathrm{sgn}(M) Y_\Delta^\infty |\tilde{m}|^{-\Delta/\beta} + Y_{2-\alpha}^\infty |\tilde{m}|^{-(2-\alpha)/\beta} + Y_2^\infty |\tilde{m}|^{-2/\beta} \pm Y_3^\infty |\tilde{m}|^{-3/\beta} + \cdots], \quad (4.16)$$

where the various coefficients are given explicitly by

$$Y_\Delta^\infty \equiv h_\infty / B^\delta Y_0^\infty |t|^\Delta, \quad (4.17)$$

$$Y_{2-\alpha}^\infty \equiv [A^\infty(\tilde{h}_\infty) + (B^2/C^+)\tilde{h}_\infty \tilde{m}_\infty(\tilde{h}_\infty)]/B^{\delta+1} Y_0^\infty, \quad (4.18)$$

$$Y_0^\infty = n_c/(m_c)^{\delta+1}, \quad (4.19)$$

$$Y_1^\infty = \frac{[m_c/B]^{1/\beta}}{k_c'}\left\{\frac{n_c'}{n_c} - (\delta+1)\frac{m_c'}{m_c}\right\}, \quad (4.20)$$

$$Y_2^\infty = \frac{[m_c/B]^{2/\beta}}{2[k_c']^2}\left\{-\frac{2(1-\alpha)}{\beta}\frac{n_c'}{n_c}\frac{m_c'}{m_c} + \frac{(\beta-\alpha)(1+\delta)}{\beta}\left(\frac{m_c'}{m_c}\right)^2 + \frac{n_c''}{n_c} - \frac{n_c'}{n_c}\frac{k_c''}{k_c'} + (1+\delta)\left(\frac{m_c'}{m_c}\frac{k_c''}{k_c'} - \frac{m_c''}{m_c}\right)\right\}, \quad (4.21)$$

where $m_c'' = m''(\theta_c)$, etc.

B. Representation of the noncritical phase

The scaling forms just discussed provide a satisfactory representation of the phases β, γ, and $\beta\gamma$ (see Fig. 1) in the vicinity of the critical line and critical endpoint, but they seem to give no account at all of the noncritical or spectator phase, α. To overcome this draw-back, Fisher and Upton [5,6] advanced a hypothesis, $\boldsymbol{\Omega}$, which asserts that as regards the singular contributions near a critical endpoint, the noncritical phase α (typically a vapor when β and γ are liquids) can be replaced by a rigid, inert wall, say ω, characterized only by a nonzero surface field h_1 favoring, say, the bulk critical phase β.

If one accepts the hypothesis $\boldsymbol{\Omega}$, one must consider a wall at, say, $z = 0$ with a corresponding wall free energy as introduced in (3.5) which, following a Landau approach [28], may be expanded as

$$f_1(M_1) = -h_1 M_1 + c_2 M_1^2 + \cdots. \quad (4.22)$$

The boundary condition (3.11) determining M_1 can be rewritten for the EdGF theory using (3.21), (3.22), and (3.25) as

$$\frac{df_1}{dM_1} = 2[W\xi^2/2\chi]_{M=M_1}^{1/2}. \quad (4.23)$$

If the surface field near bulk criticality scales as $h_1 \sim |t|^{\Delta_1}$ when $h_1 \to 0$, this relation leads to $\Delta_1 = \frac{1}{2}(2-\alpha-\eta\nu) = \mu - \beta$. However, it is known that the critical exponents for surface quantities such as h_1 and M_1 are characterized by exponents Δ_1, β_1, etc., that *cannot* be derived simply from the bulk exponents [40–42]. Hence the exponent relation implied by (4.22) for small h_1 is not, in fact, valid. However, this failure of the local functional theory is of no concern in the present situation since we wish to keep the field h_1 *fixed*

and nonzero. Hence the correct scaling combination $h_1/|\tilde{t}|^{\Delta_1}$ *diverges* when $\tilde{t}\to 0$ and hence h_1 does not appear explicitly in the asymptotic scaling forms. From our viewpoint, then, it is only necessary to investigate *large* $|h_1|$ and, correspondingly, large $|M_1|$. In a more general formulation the α phase would be represented by an extra ("third") minimum in the extended free-energy function $A^{\dagger}(M,t,g)$ at some value $M=M_\alpha(t,g)$ with, say, $M_\alpha<0$ corresponding to a vapor phase: a fuller investigation [5,6] then shows that the hypothesis **Ω** is justified within EdGF theory. Of course, the effective surface order M_1 does not become indefinitely large in this formulation: however, for the singular behavior near the critical endpoint we may imagine taking M_1 to $-\infty$, the negative sign being chosen so that, as indicated, the density ρ_α of the vapor phase lies below the critical density ρ_c (corresponding to $M=0$) so that the wall field h_1 should induce a negative value of M. This limit entails, as will now be discussed, the subtraction of appropriate leading terms that would otherwise appear as divergencies but which, in reality, contribute only to noncritical "background" terms.

C. Implications of an unbounded surface field

To use the integral expression (4.1) for the surface tension in the limit where h_1 and, hence, M_1 remain finite so that the scaled variable $\tilde{m}\sim M/|t|^\beta$ becomes large near the wall at $z=0$ when $t\to 0$, we need to examine the integrand. When $|\tilde{m}|\to\infty$ we find

$$\left[W(M)\frac{\xi^2(M)}{2\chi(M)}\right]^{1/2} = |M|^{(\mu-\beta)/\beta}(Y_0^\infty Z_0^\infty)^{1/2}\left\{1+\frac{(Y_1^\infty+Z_1^\infty)t}{2|M/B|^{1/\beta}} - \mathrm{sgn}(M)\frac{h_\infty/B^\delta Y_0^\infty}{2|M/B|^\delta}+\frac{Y_{2-\alpha}^\infty|t|^{2-\alpha}}{2|M/B|^{\delta+1}} + \frac{[4(Y_2^\infty+Z_2^\infty)-(Y_1^\infty-Z_1^\infty)^2]t^2}{8|M/B|^{2/\beta}} - \mathrm{sgn}(M)\frac{(Z_1^\infty-Y_1^\infty)h_\infty t/B^\delta Y_0^\infty}{4|M/B|^{1/\beta+\delta}} + \frac{(Z_1^\infty-Y_1^\infty)Y_{2-\alpha}^\infty t|t|^{2-\alpha}}{4|M/B|^{1/\beta+\delta+1}}+\mathcal{O}(|\tilde{m}|^{-3/\beta})\right\}. \tag{4.24}$$

On integration the leading term $|M|^{(\mu-\beta)/\beta}$ yields $|M_1|^{\mu/\beta}$ which diverges when $M_1\to-\infty$ since $\mu/\beta>0$. Similarly, the second term yields a divergence when $(\mu-1)/\beta>0$, which applies when $d>2$. The third term gives $|M_1|^{(\mu-\Delta)/\beta}$ which vanishes in the limit $M_1\to-\infty$ since $\mu<\Delta$ for $d=3$. However, when $d=4$ it diverges as $\ln|M_1|$. Higher order terms do not yield any divergencies when $M_1\to-\infty$. Hence, to remove the divergence in the integral when $M_1\to-\infty$ for $2\leqslant d\leqslant 4$, the first three terms must be subtracted.

When $M_\infty>0$ the integral in (4.1) runs through $M=0$ which is problematical because the piece to be subtracted is singular at $M=0$. To avoid this, we split the integral at an arbitrary point $M^*<0$ and make the subtraction only in the integral from M_1 to M^*: of course, the values of M^* should not affect the final results. Finally, the subtracted form of the surface tension expression (4.1) can be written

$$\Sigma(t,h_\infty;M_1) = I_1 + I_2 + I_3(M^*) - I_3(M_1) + f_1(M_1), \tag{4.25}$$

where the various contributions follow from

$$I_1 = 2\int_{M^*<0}^{M_\infty} dM[W(M)\xi^2(M)/2\chi(M)]^{1/2}, \tag{4.26}$$

$$I_2 = 2\int_{M_1}^{M^*} dM\left[\{W(M)\xi^2(M)/2\chi(M)\}^{1/2}-(Y_0^\infty Z_0^\infty)^{1/2}|M|^{\mu/\beta-1}\times\left\{1+\frac{(Y_1^\infty+Z_1^\infty)t}{2|M/B|^{1/\beta}}+\frac{h_\infty/B^\delta Y_0^\infty}{2|M/B|^\delta}\right\}\right], \tag{4.27}$$

$$I_3(M_1) = 2(Y_0^\infty Z_0^\infty)^{1/2}\int^{M_1} dM|M|^{\mu/\beta-1}\times\left[1+\frac{(Y_1^\infty+Z_1^\infty)t}{2|M/B|^{1/\beta}}+\frac{h_\infty/B^\delta Y_0^\infty}{2|M/B|^\delta}\right]. \tag{4.28}$$

The third, *indefinite* integral, which together with $f_1(M_1)$ contains all divergences in the limit $M_1\to-\infty$, can be performed analytically yielding

$$I_3(M) = -2(Y_0^\infty Z_0^\infty)^{1/2}\left[\frac{(-M)^{\mu/\beta}}{\mu/\beta}+\frac{(Y_1^\infty+Z_1^\infty)B^{1/\beta}t}{2(\mu-1)/\beta}(-M)^{(\mu-1)/\beta} + \frac{h_\infty}{2Y_0^\infty}\begin{cases}\beta(-M)^{\mu/\beta-\delta}/(\mu-\Delta), & d<4\\ \ln[(-M)/Br_\infty^\beta], & d=4\end{cases}\right], \tag{4.29}$$

where for $d=4$ we have made the argument of the logarithm dimensionless and scale-free; this is harmless because the extra $\ln(Br_\infty^\beta)$ term amounts merely to an additive constant.

D. Singular part of the surface tension

Following the discussion, we now identify the finite, singular part of the surface tension as

$$\Delta\Sigma(t,h_\infty) = I_1 + I_2 + I_3^* \quad \text{with } I_3^*\equiv I_3(M^*), \tag{4.30}$$

where the limit $M_1\to\infty$ in any remaining M_1-dependence is to be understood. Note, furthermore, that when $d<4$, the diverging parts that have been subtracted vary only linearly with t. As mentioned, they may thus be regarded as a part of the common analytic background, $\Sigma_0(T)$, for the surface tension: see (1.2) and (1.3). In identifying $\Delta\Sigma$ for $d=4$ there is some unavoidable arbitrariness associated with the introduction of the $\ln(Br_\infty^\beta)$ term: but this is of little significance.

Finally, to employ the parametric representations, we change the integration variable from M to θ in the integrals I_1 and I_2. From (1.8), we have

$$\left(\frac{\partial M}{\partial\theta}\right)_t = \mathrm{sgn}(t)\frac{k(\theta)m'(\theta)-\beta k'(\theta)m(\theta)}{|k(\theta)|^{\beta+1}}|t|^\beta \tag{4.31}$$

and on defining $\theta^*<0$ via

$$M^*/|t|^\beta = m(\theta^*)/|k(\theta^*)|^\beta \tag{4.32}$$

we find

$$I_1 = 2\,\mathrm{sgn}(t)|t|^{\mu}\int_{\theta^*}^{\theta_\infty} d\theta \frac{k(\theta)m'(\theta) - \beta k'(\theta)m(\theta)}{|k(\theta)|^{\mu+1}}\sqrt{a_\infty(\theta)w(\theta)}, \tag{4.33}$$

$$I_2 = 2\,\mathrm{sgn}(t)|t|^{\mu}\int_{-\theta_c}^{\theta^*} d\theta \frac{k(\theta)m'(\theta) - \beta k'(\theta)m(\theta)}{|k(\theta)|^{\mu+1}}\Bigg[\sqrt{a_\infty(\theta)w(\theta)} - (Y_0^\infty Z_0^\infty)^{1/2}|m(\theta)|^{\mu/\beta-1}\Bigg\{1 + \frac{(Y_1^\infty + Z_1^\infty)k(\theta)}{2|m(\theta)/B|^{1/\beta}} + \frac{Y_\Delta^\infty |k(\theta)|^{\Delta}}{2|m(\theta)/B|^{\delta}}\Bigg\}\Bigg], \tag{4.34}$$

where $w(\theta)$ is given by (4.11) (for fixed θ_∞), while $I_3(M^*)$ can be written as

$$I_3^* = -2(Y_0^\infty Z_0^\infty)^{1/2}|t|^{\mu}B^{\mu/\beta}(y^*)^{-\mu}\Bigg[\frac{\beta}{\mu} + \mathrm{sgn}(t)\frac{(Y_1^\infty + Z_1^\infty)y^*}{2(\mu-1)/\beta} + \frac{Y_\Delta^\infty}{2}\begin{cases}\beta(y^*)^{\Delta}/(\mu-\Delta), & d<4\\ \beta(y^*)^{\mu}\ln(|k_\infty|/y^*), & d=4\end{cases}\Bigg], \tag{4.35}$$

where $y^* = |k(\theta^*)|[-m(\theta^*)/B]^{-1/\beta}$. It is to be understood that, below T_c, the integral I_1 must be interpreted as $\int_{\theta^*}^{\theta_\infty} = \int_{\theta^*}^{-\theta_0} + \int_{\theta_0}^{\theta_\infty}$ since, by our periodic parametric construction, $\theta = +\theta_0$ and $\theta = -\theta_0$ are identified together with $M = 0$.

These expressions for I_1, I_2, and I_3^* together with (4.30) for $\Delta\Sigma(t, h_\infty)$ constitute our explicit results for the singular part of the surface tension. Note that M_1, the boundary value of the profile on the wall that stands in for the α phase, does *not* enter these expressions. On the other hand the arbitrary value θ^* does appear; however, the total $I_1 + I_2 + I_3^*$ should be independent of θ^* and this may be checked in explicit calculations.

V. PARAMETRIC SCALING FUNCTION FOR $d=3$

In this section we examine the numerical results for the parametric scaling function $s(\theta)$ introduced in (1.12) that follow from the EdGF surface tension expressions obtained in the previous section, specifically (4.30) with (4.33)–(4.35).

A. Numerical evaluation of the scaled tension

Now given the parametric angular functions $k(\theta)$, $m(\theta)$, etc., the numerical integration of I_1 in (4.33) can be performed readily. However, there is an endpoint singularity in I_2 in (4.34) at $\theta = -\theta_c$ where $k(\theta)$ vanishes. On using the expansion (4.24) for $[W\xi^2/2\chi]^{1/2}$ one sees that the singularity has the form $|\theta - \theta_c|^{\phi}$ with $\phi = 1 - \alpha - \mu = \nu - 1 < 0$ for $d=3$. Although divergent, this singularity is integrable and can be handled by standard techniques [43].

As a check on the numerical calculations, it is useful to recall the mean-field limit for which exact analytic results can be obtained. Indeed, from the asymptotic classical equation of state, namely,

$$h(M,t) = DM(B^2 t + M^2) \qquad \text{with} \qquad D = 1/B^2 C^+, \tag{5.1}$$

one can find the auxiliary free energy via (2.6) to obtain

$$W(M) = \tfrac{1}{2}tB^2 D(M^2 - M_\infty^2) + \tfrac{1}{4}D(M^4 - M_\infty^4) - h_\infty(M - M_\infty), \tag{5.2}$$

in which $M_\infty = M(T, h_\infty)$ is, of course, the appropriate bulk equilibrium value. Using the EdGF formulation and taking $\xi^2/2\chi = \frac{1}{2}J_0$ [see (2.8)], the critical surface tension can be calculated analytically, yielding

$$\Sigma_{\beta|\gamma} = 2\int_{-M_0(T)}^{M_0(T)} dM[W(M)\xi^2/2\chi]^{1/2} = \tfrac{2}{3}\sqrt{2J_0/B^2C^+}M_0^3(T), \tag{5.3}$$

from which the amplitude K defined in (1.1) is

$$K = \tfrac{2}{3}K_0 \qquad \text{with} \qquad K_0 = \sqrt{2J_0B^4/C^+}. \tag{5.4}$$

Similarly, the amplitudes $K^{\pm}$ for the noncritical surface tension can be calculated using the subtraction scheme discussed above; they are found to be

$$K^+ = -\tfrac{1}{3}\sqrt{2}K_0, \quad K^- = \tfrac{1}{3}K_0, \tag{5.5}$$

which values confirm the universal amplitude ratios P and Q stated in (1.6).

For the numerical results presented below we have used the extended sine model expounded in [9], specifically in Eqs. (5.6) and (7.4) with (6.1) and (4.4). The numerical parameter values for $d=3$ are given in Eqs. (6.2) and (7.5) of Ref. [9]. In light of more recent estimates for the critical exponents and universal amplitude ratios of $d=3$ Ising models [44–46], the model parameters should, ideally, be updated. However, the resulting changes could induce only rather small effects. Thus the new estimates $\nu \simeq 0.6302$ and $\gamma \simeq 1.2375$ [45] differ from the adopted values of [9] by only 0.16% and 0.28%, respectively. The universal amplitude ratio estimates $f_1^+/f_1^- = 1.963 \pm 8$ and $C^+/C^- = 4.762 \pm 8$ [45] agree well with those used in [9] lying within the uncertainty ranges although their central values are shifted by 0.15% and 3.8%, respectively. Furthermore, it has been shown via parameter-sensitivity checks that the associated variations in universal ratios are less than 5% [9]. Thus the accepted parameter values from [9] are perfectly reasonable for the numerical aspects of the calculations reported here.

The computation may be set up to generate the mean-field results applicable when $d>4$: see Appendix D of Ref. [17] for the appropriate parameter values. Our numerical values for the mean-field case agree up to eight digits and the lack of any dependence on θ^* was verified. [For convenience the values $\theta^* = -3\theta_c/4$ for $0 \leqslant \theta_\infty < \theta_c$ and $\theta^* = -(\theta_c + \theta_0)/2$ for $\theta_c < \theta_\infty \leqslant \theta_0$ were adopted [17].] In $d=3$ dimensions the

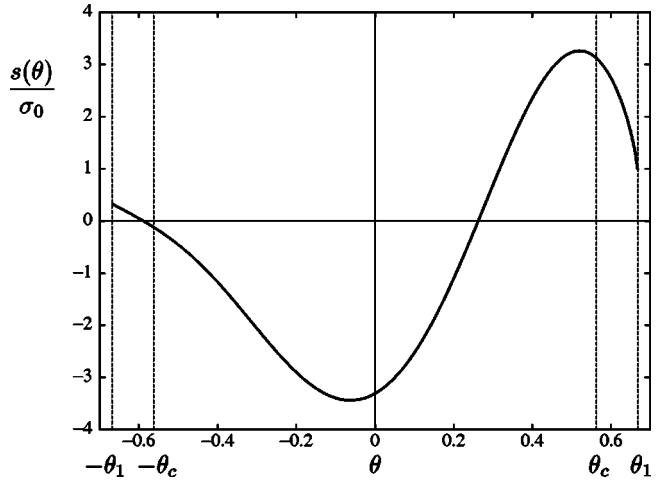

FIG. 2. The angular scaling function $s(\theta)$ for the surface tension in $d=4$ dimensions as given by EdGF theory. Some significant numerical values are $\theta_c \simeq 0.562\,345$ and $\theta_1 \simeq 0.667\,708$ corresponding to $s_c/\sigma_0 = 3.120\,23$, $s_{-c}/\sigma_0 = -0.122\,322$, $s_1/\sigma_0 = 0.976\,225$, and $s_{-1}/\sigma_0 = 0.325\,408$. Note also $s(0)/\sigma_0 = -3.306\,20$ [17].

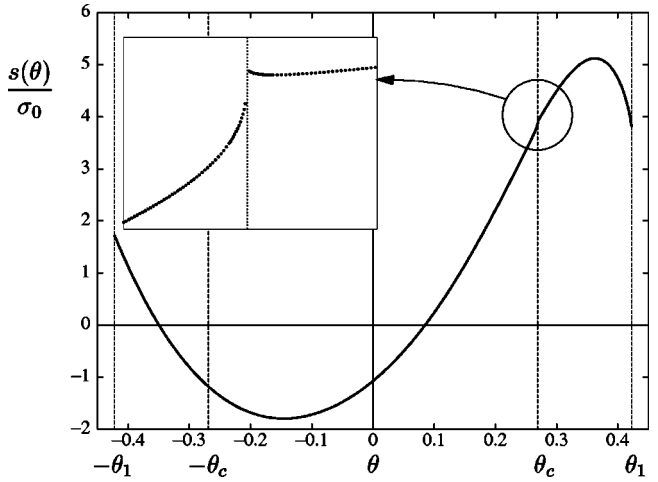

FIG. 3. The calculated angular function for the surface tension in $d=3$ dimensions based on EdGF theory and the extended sine model [9]. The inset clearly shows a cusp at $\theta=\theta_c$ (i.e., at $T=T_c$ for $h_\infty>0$) with a corresponding value $s_c/\sigma_0 = 3.91731$. The values of s_{-c} and $s_{\pm 1}$ are entered in Table I.

value of θ^* was varied from -0.05 to -0.26 for a sample value of θ_∞ near θ_c: no change in $s(\theta)$ was found within eight-digit precision.

B. Calculated scaling functions

Our calculations may be summarized by presenting the angular function $s(\theta)$ for the surface tension. For the purpose of normalization, we employ

$$\sigma_0 = (a_\infty l_0 m_0^3)^{1/2}, \tag{5.6}$$

which has the same units as surface tension. Figure 2 presents a plot of $s(\theta)$ for $d=4$. One sees that, owing to the wall dependence (embodied in $M_1 \to -\infty$), $s(\theta)$ is *not* symmetric with respect to $\theta=0$. Notice also that $s(\theta)$ varies perfectly smoothly across the critical isotherm values $\theta=\pm\theta_c$ as it should.

The qualitative features of the scaling function in $d=3$ dimensions are the same as for $d=4$. However, as seen in Fig. 3, an unexpected, albeit small cusp appears at $\theta=\theta_c$. The presence of the cusp (which is certainly absent when $d=4$) implies that there is a line of nonanalyticity along the critical isotherm $\tilde{t}=0$ when $h_\infty>0$. This is quite unphysical since singularities in the thermodynamic functions, including surface quantities, can occur only at the critical point $(t,h_\infty)=(0,0)$. Thus, from the analyticity away from the critical point, one expects

$$\Delta\Sigma(t,h_\infty) = \Delta\Sigma_c(h_\infty) + \Delta\Sigma_1^{\pm}(h_\infty)t + \Delta\Sigma_2^{\pm}(h_\infty)t^2 + \cdots, \tag{5.7}$$

when $h_\infty \neq 0$ and $t \to 0\pm$, respectively. However, analysis shows that the surface tension predicted by the EdGF theory behaves as

$$\Delta\Sigma(t,h_\infty) = \Delta\Sigma_c(h_\infty) + \Delta\Sigma_{1/2}^{\pm}(h_\infty)|t|^{\mu-1+\alpha/2} + \Delta\Sigma_1^{\pm}(h_\infty)|t|^{\mu+1-\alpha/2-\Delta} + \cdots, \quad h_\infty > 0, \tag{5.8}$$

when $t \to 0\pm$: see Appendix A in Ref. [17]. In $d \geqslant 4$ one has $\mu - 1 + \frac{1}{2}\alpha = \frac{1}{2}$ so one should, in principle, see a square root cusp then; but such a cusp is absent in Fig. 2. This is because the amplitudes $\Delta\Sigma_{1/2}^{\pm}(h_\infty)$ vanish identically in the classical situation: see Eq. (A.30) of Ref. [17].

It transpires, as we will now explain, that this erroneous singular behavior appears because the EdGF theory does not satisfy the desideratum **I** of Sec. III. More specifically, a zero of the order parameter profile is not represented correctly when $T \simeq T_c$ and $h_\infty > 0$: recall that the order parameter in the EdGF surface tension integral (4.1) now runs from $M=M_1<0$ to $M=M_\infty>0$ and so passes through the value $M=0$ which is critical when $T=T_c$ or $\theta=\theta_c$. Equivalently, the EdGF surface tension can be represented by a real-space integral involving the free energy $W[M(z)]$, as in (3.26). Now, let us focus on the term $h_\infty M(z)$ in $W(M)$ [see (2.5)]; i.e., consider the contribution of $\int dz\, h_\infty M(z)$ to the surface tension. In order to find the scaling behavior of the profile near $M=0$, we may analyze (3.25) to find (see Appendix B of Ref. [17] for details)

$$M(z) \propto t^{\eta\nu/2}(z - z_0), \tag{5.9}$$

when $z \to z_0$. Evidently the z-dependence is linear as expected from the analyticity of $M(z)$ when $t \neq 0$. However, by scaling z varies as $\xi \sim t^{-\nu}$ and h_∞ as t^Δ; thus the scaling behavior of the profile $M(z)$ near $z=z_0$ can be estimated leading to

TABLE I. Numerical values for the ameliorated angular surface tension scaling function $\overline{s}(\theta)$ in three dimensions. Note that $\theta_c = 0.269\,293$ and $\theta_1 = 0.422\,519$ [9].

θ	$\overline{s}(\theta)/\sigma_0$	θ	$\overline{s}(\theta)/\sigma_0$	θ	$\overline{s}(\theta)/\sigma_0$	θ	$\overline{s}(\theta)/\sigma_0$
$-\theta_1$	1.727 13	−0.20	−1.677 43	0.08	−0.076 19	0.30	4.458 74
−0.40	1.125 36	−0.16	−1.783 25	0.12	0.587 32	0.32	4.792 82
−0.36	0.207 79	−0.12	−1.767 07	0.16	1.355 90	0.34	5.022 93
−0.32	−0.513 65	−0.08	−1.638 86	0.20	2.210 93	0.36	5.121 25
−0.28	−1.055 67	−0.04	−1.405 58	0.24	3.129 71	0.38	5.049 63
$-\theta_c$	−1.173 07	0	−1.069 44	$+\theta_c$	3.812 64	0.40	4.739 23
−0.24	−1.438 71	0.04	−0.627 87	0.28	4.050 87	$+\theta_1$	3.806 99

$$\int dz\, h_\infty M(z) \sim t^{\eta\nu/2}\xi^2 h_\infty \int \frac{dz}{\xi}\frac{(z-z_0)}{\xi} \sim t^{(\eta\nu/2)-2\nu+\Delta}. \tag{5.10}$$

Note that the second integral is dimensionless and scale-free and so has been regarded as a fixed number. Via the scaling relations, the exponent $(\eta\nu/2)-2\nu+\Delta$ reduces to $\mu-1+(\alpha/2)$ which corresponds to the cusp appearing in (5.8).

Since the correct scaling function should not exhibit such nonanalyticity, we introduce an interpolation procedure that smooths out the calculated cusp in $s(\theta)$. The θ range, say $[\theta_a, \theta_b]$, selected for the interpolation is arbitrary. However, the choice $(\theta_a, \theta_b) = (0.20, 0.35)$ encompasses the cusp and seems reasonable. We have used a polynomial $P(\theta)$ of degree 5 which is the minimal order to match the first and second derivatives at both ends of this interval. The resulting polynomial for the extended sine model parameters is given in Eq. (4.4.50) of [17]. It agrees closely with the calculated values of $s(\theta)$ in the intervals [0.20, 0.26] and [0.32, 0.35]; furthermore, the largest deviation of $P(\theta)$ from $s(\theta)$ occurs at the cusp and is only 3%.

From now on, when the distinction matters, we will write $\overline{s}(\theta)$ for the ameliorated angular function to distinguish it from $s(\theta)$ that has the cusp at $\theta = \theta_c$. Selected numerical values of $\overline{s}(\theta)$ are given in Table I; values spaced at intervals $\Delta\theta = 0.01$ are available in Table 4.1 of [17].

In the previous study of the extended sine model [9], various parameter sets near the preferred set in Eq. (6.2) of [9] were examined in order to check the sensitivity of the universal amplitude ratios. Here, we also check the sensitivity of $s(\theta)$ under the variations in the parameter sets considered in Table I of [9]. As explained in Sec. VII of [9], the optimal parameters $a_{\infty 0}$, $a_{\infty 2}$, etc., for the true correlation length are determined separately for each set by fitting the universal ratios $K(f^-)^2$ and $\alpha A^+(f^+)^d$, f^+/f^-, and $(C^+/C^c)(f^c/f^+)^{2-\eta}$. Then $s(\theta)$ is computed for each parameter set using EdGF theory.

It must be noted that the value of θ_1 depends somewhat on the parameter set. This implies that the values of $s(\theta)$ calculated from different parameter sets are not strictly comparable. However, the change in θ_1 occurs only in the third decimal place. Thus, ignoring the small changes in the θ scale, we have examined $\Delta s(\theta) \equiv s(\theta) - s(\theta)_0$, i.e., the deviations of $s(\theta)$ calculated using the sets 1, 2, …, 6 in Table I of [9] in place of the preferred set (6.2) of Ref. [9].

The largest deviation occurs at $\theta = \theta_1 \simeq 0.42$; normalized by the value $\overline{s}(\theta_1)$ in Table I it is about 3%. In [9] the variations in the predicted universal ratios associated with the parameter changes ranged from 0.2% to 5%. Thus, the function $s(\theta)$ shows only the same level of variation as might have been anticipated.

Finally, we have also checked the effects on $s(\theta)$ of using "untuned" estimates for $a_\infty(\theta)$. Indeed it was found in [9] that the $[2/0]$ Padé approximant for $a_\infty(\theta)$ could not fit the universal ratio while also fitting f^+/f^-, $\alpha A^+(f^+)^3$, and $(C^+/C^c)(f^c/c^+)^{2-\eta}$. Likewise for the other approximants of the same order, namely, $[1/1]$ and $[0/2]$. Hence, it was necessary to introduce the $[3/0]$ approximant. By using the $[2/0]$ approximant for $a_\infty(\theta)$, which is representative of the low-order approximants, we have calculated the angular function $s(\theta;[2/0])$ with the preferred parameter set (6.2) of [9]. The difference between $s(\theta;[2/0])$ and $s(\theta;[3/0])$ in the range $-\theta_1 \leqslant \theta \leqslant \theta_c$ is very small; indeed, it is invisible on a plot. However, a large difference of about 30% arises in the subcritical range $\theta_c \leqslant \theta \leqslant \theta_1$. This occurs (i) because the approximants $[2/0]$ and $[3/0]$ behave quite differently in the two-phase region $\theta_1 \leqslant |\theta| \leqslant \theta_0$ (see Fig. 8 of [9]) and (ii) because the calculation of $s(\theta_\infty)$ for $\theta_c < \theta_\infty < \theta_1$ involves integration through the two-phase region whereas the range $-\theta_1 \leqslant \theta_\infty < \theta_c$ requires integration only through the one-phase region in which the approximants are very similar.

VI. NUMERICAL RESULTS FOR THE SURFACE TENSIONS

Based on the angular scaling function $s(\theta)$ or, where appropriate, the ameliorated version $\overline{s}(\theta)$, calculated with the preferred parameter set (6.2) and (7.5) of Ref. [9], we now describe various theoretical predictions for the interfacial tension near a critical endpoint.

A. Amplitude ratios

Recall first the surface tension amplitudes $K^\pm$ and K defined in (1.1)–(1.3). On using the parametric form for $\Delta\Sigma$ in (1.12) the surface tension amplitude above T_c is readily read off as

$$K^+ = s(0)/[k(0)]^\mu = s(0). \tag{6.1}$$

Owing to the asymmetry of $\overline{s(\theta)}$ with respect to $\theta \gtrless 0$, we must choose the sign of $\pm\theta_1$ appropriately for zero-field below T_c. In accord with Fig. 1(a), the $\alpha|\beta$ interface exists beneath T_c when $h \lessgtr 0$; thus, the amplitude K^- must be evaluated at $\theta = -\theta_1$ yielding

$$K^- = s(-\theta_1)/|k(\theta_1)|^\mu. \tag{6.2}$$

Similarly, at $\theta = \theta_1$ one obtains the amplitude for $\Delta\Sigma_{\alpha|\gamma}$ in the limit $h \to 0+$, which via Antonow's rule is the sum $(K+K^-)$: thus we have

$$K = [s(\theta_1) - s(-\theta_1)]/|k(\theta_1)|^\mu. \tag{6.3}$$

It is also instructive to define corresponding critical surface tension amplitudes *on* the critical isotherm. Via scaling one can write

$$\Delta\Sigma \approx K^c_{\gtrless}|h|^{\mu/\Delta} \approx K^{\gtrless}_M |M|^{\mu/\beta}, \tag{6.4}$$

where the sub- and superscripts $>$ and $<$ stand for $h, M > 0$ and $h, M < 0$, respectively: owing to the asymmetry of the surface tension with respect to $h \to -h$, this distinction is essential. For reference we may note that $\mu/\Delta \simeq 0.80_6$ while $\mu/\beta = 3.8_5$. The parametric representations then yield

$$K^c_> = \overline{s(\theta_c)}/|l(\theta_c)|^{\mu/\Delta}, \quad K^c_< = s(-\theta_c)/|l(\theta_c)|^{\mu/\Delta}. \tag{6.5}$$

Note the appearance of $\overline{s(\theta)}$ here so that the prediction for $K^c_>$ depends on the amelioration procedure.

The specific reduced surface tension amplitudes predicted by our EdGF theory with the extended sine model are thence

$$\begin{gathered} K^+/\sigma_0 = -1.069\,44, \quad K^-/\sigma_0 = 1.281\,68, \quad K/\sigma_0 = 1.543\,44, \\ K^c_>/\sigma_0 l_0^{-\mu/\Delta} = 0.293\,755, \quad K^c_</\sigma_0 l_0^{-\mu/\Delta} = -0.090\,382\,6, \\ K^>_M/\sigma_0 m_0^{-\mu/\beta} = 923.242, \quad K^<_M/\sigma_0 l_0^{-\mu/\beta} = -284.063, \end{gathered} \tag{6.6}$$

where we used Table I for the $\overline{s(\theta)}$ values and the extended sine model values [9]

$$\begin{gathered} k(\theta_1) = -1.266\,16, \quad l(\theta_c)/l_0 = -l(-\theta_c)/l_0 = 0.529\,162, \\ m(\theta_c)/m_0 = -m(-\theta_c)/m_0 = 0.240\,366, \end{gathered} \tag{6.7}$$

while σ_0 is defined in (5.6) and represents the nonuniversal surface tension scale.

From Eq. (6.6), one obtains the universal amplitude ratios

$$P = 0.137_5 \pm 2, \quad Q = -0.834 \pm 2, \tag{6.8}$$

where the uncertainties have been estimated by examining results from the other parameter sets in Table I of Ref. [9]. In comparison with the preliminary calculations quoted in (1.7), one sees that our improved estimate for P is about 15% larger [and still *positive* in contrast to (1.6)] while the Q value displays only a 0.5% deviation. These estimates will be discussed elsewhere [22] in relation to the experimental observations of Mainzer-Althof and Woermann [20].

For the surface tensions on the critical isotherm, our analysis generates the universal amplitude ratio predictions

$$\begin{gathered} \frac{K^c_>}{K}\left(\frac{B}{C^+}\right)^{\mu/\Delta} = 3.34 \pm 4, \quad \frac{K^>_M}{K} B^{\mu/\beta} = 5.26 \pm 7, \\ \frac{K^c_<}{K}\left(\frac{B}{C^+}\right)^{\mu/\Delta} = -1.02_9 \pm 1, \quad \frac{K^<_M}{K} B^{\mu/\beta} = -1.62 \pm 2, \end{gathered} \tag{6.9}$$

where we recall that B and C^+ are defined as in [8]. More directly we find

$$K^c_>/K^c_< = K^>_M/K^<_M = -3.25 \pm 5, \tag{6.10}$$

which may also be used in analyzing experimental data and might well be tested in simulations of Ising-type systems.

We plan, as mentioned in the Introduction, to consider the applications of the present theory to experiments in the future [22]; but it should be noted here that the difference in sign and magnitude of the amplitudes $K^>_M$ and $K^<_M$ was explicitly remarked by NWW on the basis of the theory of Ramos-Gómez and Widom [10], a square-gradient approach formulated to incorporate $\delta = 5$. [See also Rowlinson and Widom [1] (pp. 287–293) and our comments following (1.4) and (2.10) above.] Furthermore, their analysis leads to $K^>_M/K^<_M \simeq -148/42 \simeq -3.5_2$; see [10] p. 614 and [1] Eq. (9.124). This value is only some 8% larger in magnitude than found here.

B. Scaling functions

While parametric scaling forms are conceptually and computationally effective, direct scaling representations, as in (1.12), are more useful for comparison with existing or proposed observations. Thus from the angular function $\overline{s(\theta)}$ we have computed the scaling functions $S_\pm(\tilde{h})$: in Fig. 4(a) these are plotted in terms of the field (or chemical potential) variable $\tilde{h}$.

In experiments, for example on binary mixtures, the density deviation ($\propto M$) is more readily accessible than the chemical potential deviation ($\propto \tilde{h}$). Hence, in practice scaling plots in terms of $\tilde{m}$ are more convenient: the corresponding scaling functions may be defined via

$$\Delta\Sigma \approx K|t|^\mu S^\pm_M(\tilde{m}) \quad \text{with } \tilde{m} = M/B|t|^\beta, \tag{6.11}$$

while their behavior is shown in Fig. 4(b). The normalizations adopted in (1.12) and here lead, with Antonow's rule (1.4), to the "jump conditions"

$$S_-(0+) - S_-(0-) = S^-_M(1) - S^-_M(-1) = 1, \tag{6.12}$$

that enter below T_c.

Away from the critical point, all bulk and surface quantities must be analytic unless some phase boundary intervenes. This is reflected in the smooth behavior of $S_+(\tilde{h})$ for all $\tilde{h}$. In contrast, there is a jump in $S_-(\tilde{h})$ at $\tilde{h} = 0$ in accordance with (6.12): for $\tilde{h} \neq 0$, however, $S_-(\tilde{h})$ is analytic for all $\tilde{h}$. Similar considerations apply to the break in the $S^-_M(\tilde{m})$ plot seen in Fig. 4(b). On the critical isotherm $T = T_c$ the two branches of the scaling function, $S_+(\tilde{h})$ and $S_-(\tilde{h})$, must join smoothly when $\tilde{h} \to \pm\infty$; this again is a consequence of the overall

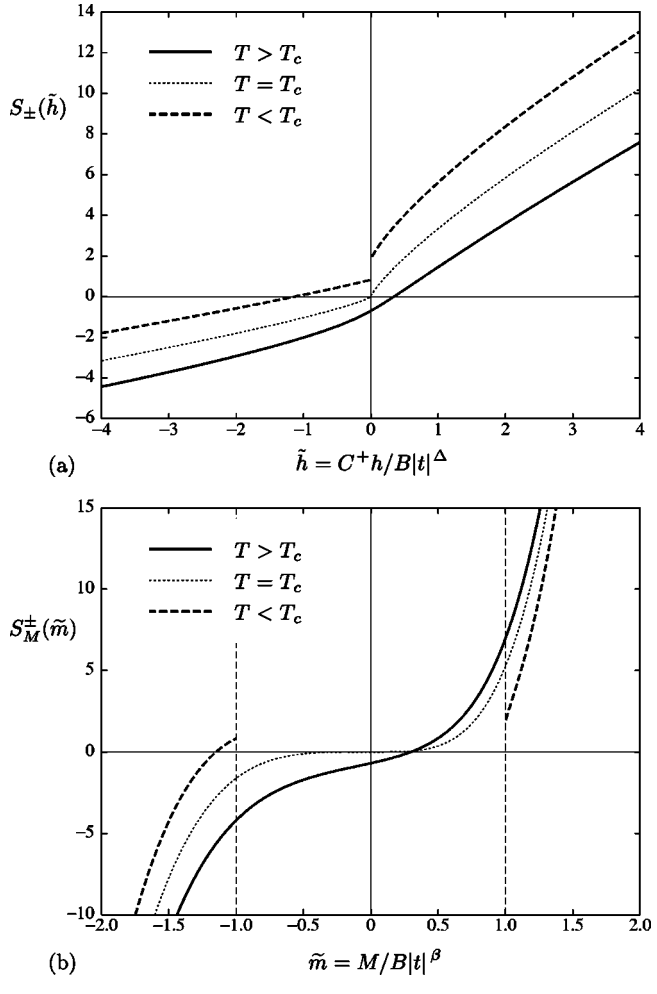

FIG. 4. The universal scaling functions predicted by the EdGF surface tension theory (a) vs the ordering field $\tilde{h}$ and (b) vs the order parameter $\tilde{m}$. Note the lack of symmetry about $\tilde{h}=\tilde{m}=0$ and the jumps dictated by (6.12).

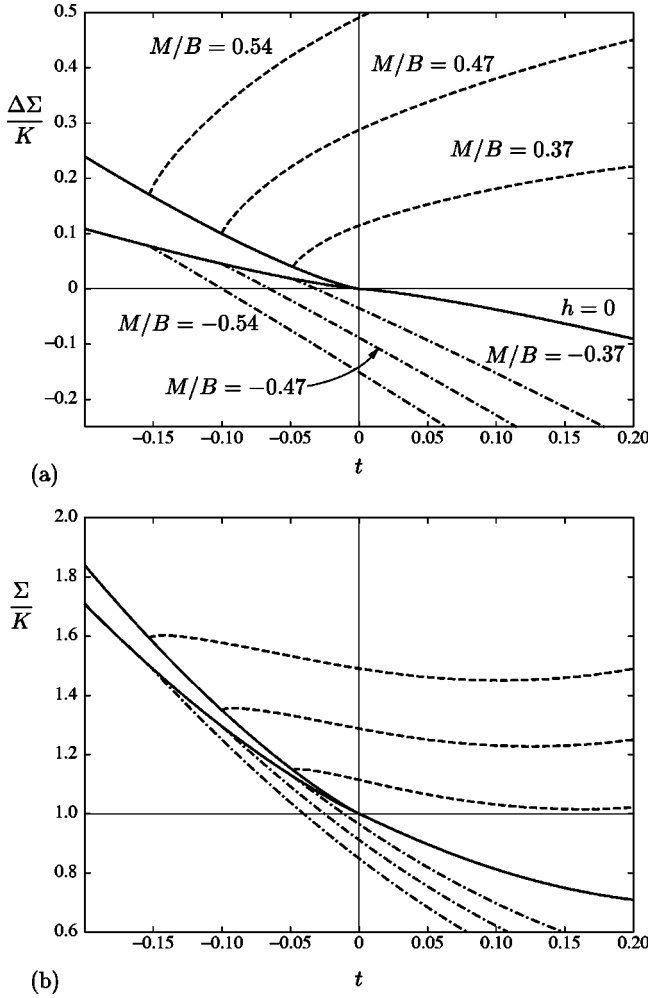

FIG. 5. Plots of (a) the singular part of the critical endpoint surface tension as a function of the reduced temperature t for fixed values of M and (b) with the addition of the model background term $\Sigma_0(T,h)$ given in (6.13) for the same values of M.

requirement of analyticity away from the phase boundary. Hence, the two branches of $S_\pm(\tilde{h})$ and $S_M^\pm(\tilde{m})$ must both asymptotically approach one another when $\tilde{h}\to\pm\infty$ and $\tilde{m}\to\pm\infty$: this can be seen easily in Fig. 4(b). Notice that the dotted line plots labeled $T=T_c$ in Fig. 4 depict only the asymptotic power-law behavior embodied in (6.4) that corresponds in these scaled plots to $\tilde{h}\to\pm\infty$. (It may also be remarked that the unphysical cusp in the EdGF surface tension on the critical isotherm for $h>0$ is located at $\tilde{h}\to+\infty$; thus, with or without the cusp, the scaling plots in Fig. 4 look similar.)

Finally, it should be clear that the scaling function plots in Fig. 4 may also be read as describing the variation of $\Delta\Sigma(T,h)\propto S_\pm(\tilde{h})=S_M^\pm(\tilde{m})$ with h and M at fixed values of $T \gtrless T_c$. In particular, one may then notice that the isotherms of $\Delta\Sigma$ vs M for T above T_c will *cross* the critical isotherm when M is positive, and, by continuity, hence also cross one another [22]. This crossing of the surface tension isotherms above T_c has been anticipated theoretically by Ramos-Gómez and Widom ([10]: see text after their Eq. (3.15) and Table I) who also point to some experimental evidence of crossings.

On the other hand the isotherms of $\Delta\Sigma$ vs $[h-h_0(T,g)]$ (which, recalling (4.2) et seq., should replace h in the figure) do *not* cross: see also Fig. 4.10 of [17]. However, in addition to the displacement $h_0(T,g)$, inclusion of the surface tension background $\Sigma_0(t,h)$ will distort naive expectations based on Fig. 4 when real isotherms for the total interfacial tension are examined vs density or chemical potential. See Fig. 5(b) below for another aspect of this issue.

It is appropriate to mention here that in their theoretical analysis of a binary fluid mixture, NWW [14] tacitly *assumed* symmetry in the surface tension above and below T_c by supposing $S_M^+(\tilde{m})=S_M^-(\tilde{m})$: see their Eqs. (2.8) and (2.9) and Figs. 3 and 10. However, on physical grounds such a symmetry is quite implausible. Thus, below T_c there are two distinct fluid phases β and γ favored by $h>0$ and $h<0$, respectively, and a vapor phase α (or wall) favoring the β phase; but, above T_c, there is only one fluid phase $\beta\gamma$: see Fig. 1. Hence, one must allow for the $T\gtrless T_c$ symmetry breaking differences seen in Fig. 4. For comparison, one may

recall that for the bulk equation of state when expressed in terms of $\tilde{m}$ (or in terms of $\tilde{h}$) one also needs *two* scaling functions, say $Q_{\pm}(\tilde{m})$ for $t \geqslant 0$ and $t \leqslant 0$, as is well known; and, again, the two branches must be analytically related. However, in the bulk thermodynamics one may accept full asymptotic symmetry under $\tilde{h} \Leftrightarrow -\tilde{h}$ or $\tilde{m} \Leftrightarrow -\tilde{m}$ and then employ just a single function, say, in terms of the variable $t/|m|^{1/\beta} \propto \tilde{m}^{-1/\beta}$. But that symmetry is also *not* applicable to the surface tension.

Experimentally, binary mixtures are prepared at various fixed compositions and the surface tension may then be observed as a function of temperature: see, e.g., [18]. This is comparable to keeping the order parameter M fixed. Accordingly we present such plots for the EdGF predictions in Fig. 5.

It must be recalled, however, that EdGF theory yields only the scaling or singular part of the surface tension. Since the leading power-law of the surface tension, $|t|^{\mu}$, vanishes at the critical point, the contribution from the analytic background is *non-negligible*. To illustrate this point, we include in Fig. 5(b) plots for the full surface tension, $\Sigma = \Delta\Sigma + \Sigma_0$, with an *assumed* but reasonably realistic *model* background term, namely,

$$\Sigma_0(T,h)/K = 1 - 2t + 5t^2, \tag{6.13}$$

where, for simplicity, only the temperature dependence has been considered. Since $K^+ < 0$ [see (6.6)], the scaling part of the surface tension above T_c in zero-field, namely, $\Delta\Sigma_{\alpha|\beta\gamma} \approx K^+|t|^{\mu}$, curves downwards as seen in Fig. 5(a). However, in Fig. 5(b), the corresponding curvature in the full surface tension now appears to be *upwards* owing to the effects of the background $\Sigma_0(T)$. In fact, the same sign of apparent curvature is observed in the NWW experiment on isobutyric acid and water [14]; this clearly demonstrates the importance of the background $\Sigma_0(T,h)$. The significance of also introducing integral powers of $\tilde{h}$ in (6.12) will be discussed elsewhere [22].

C. The complete-wetting singularity

It has been predicted by Cahn [26] that a logarithmic singularity should occur in the slope of $\Delta\Sigma_{\alpha|\gamma}(T,h)$ on approaching the coexistence curve below T_c, i.e., by taking $\tilde{h} \to 0+$ (along any generic, nontangential path). This logarithmic singularity is associated with the complete-wetting transition that, in turn, is reflected in Antonow's rule. Recall that when $\tilde{h}=0$, the two liquid phases β and γ coexist with the vapor phase α. Thus, when $\tilde{h} \to 0+$ while α and γ phases coexist [i.e., on the surface σ in Fig. 1(a)], the β phase of intermediate density emerges and spreads over (or wets) the $\alpha|\gamma$ interface. Indeed, one can explicitly show that such a singularity arises within the EdGF theory: see Appendix C of [17]. The analysis establishes that the coefficient of the $\ln \tilde{h}_{\infty}$ term in $(\partial\Delta\Sigma/\partial\tilde{h})$ is positive, which is fully consistent with the numerical calculations presented in Fig. 6: these demonstrate a $\ln(T-T_0)^{-1}$ singularity in the derivative of the surface tension when T approaches the coexistence curve at fixed density $\rho > \rho_c$, i.e., $M > 0$.

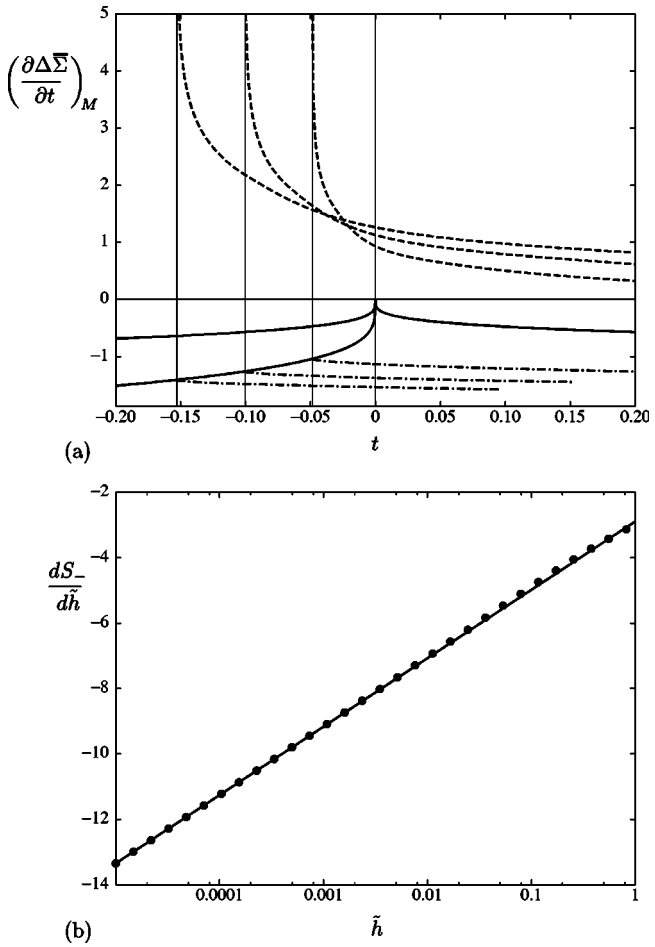

FIG. 6. (a) Temperature derivative of $\Delta\bar{\Sigma} \equiv \Delta\Sigma/K$ at fixed M (with values the same as in Fig. 5) revealing a logarithmic singularity when M is positive and t (<0) approaches the coexistence curve; (b) semilogarithmic plot of the derivative of the scaling function $S_-(\tilde{h})$ beneath T_c: the straight line is a guide to the eyes while the dots represent the derivative.

Although the presence of a logarithmic singularity in $\Sigma_{\alpha|\gamma}(h)$ on approaching a wet interface may be regarded as well established theoretically, an important caveat is that in all cases the corresponding theoretical analysis entails the assumption that interactions within the fluids are entirely of a short-range character, i.e., decaying faster than any power-law. This, of course, precludes slowly decaying interaction potentials such as the $1/r^6$ form that characterizes the van der Waals intermolecular forces prevalent in real molecular fluids. At fixed temperature T in the range $T_W < T < T_c$ van der Waals forces should generate a $(h-h_0)^{-1/3}$ singularity in $\Sigma_{\alpha|\gamma}(h)$. Thus, without special allowance for power-law potentials, a local functional analysis such as our EdGF theory must be suspect in relation to real fluid systems unless short range interactions happen to dominate for, say, reasons of symmetry, or accidental near-cancellation, etc.

On the other hand, in the case of $d=3$ bulk critical behavior it is known that $1/r^6$ potentials enter the asymptotic scaling forms only as *irrelevant* corrections-to-scaling (even though these may be *dangerously irrelevant* for certain quantities such as correlation functions at long distances) [47]. It

is possible that a similar situation pertains in the case of the surface tensions near a critical endpoint in which case a local functional theory might still prove asymptotically adequate. To our knowledge, however, this issue remains open and, as yet, a singularity in the derivative of the surface tension $\Sigma_{\alpha|\gamma}(T,h)$ near a critical endpoint has not been identified experimentally: see, e.g., [14].

VII. SUMMARY

As illustrated in Fig. 1, binary fluid mixtures exhibit critical endpoints where, in the three-dimensional thermodynamic field space, a critical line of mixing transitions terminates at a first-order transition surface between the liquid phases and their common vapor phase. At such critical endpoints, the interfacial or surface tension $\Sigma(T,h)$ becomes singular in both temperature and ordering field h. Our aim here has been to calculate the scaling functions describing the asymptotic behavior of the surface tensions through the whole neighborhood of the critical endpoint.

To this end, the local functional theory of Fisher and Upton [5,6] in the extended de Gennes–Fisher (EdGF) version of the theory, has been exploited because it captures many significant physical features tied to the nonclassical values of the relevant critical exponents, especially $\eta > 0$. As seen in (4.1), the EdGF theory requires suitable scaling representations for the auxiliary free energy $W(M;T,h_\infty,g)$ and for the correlation length factor $\xi^2/2\chi$. To generate these, we have used the extended sine model of Ref. [9], since it embodies the appropriate analytic behavior, extends smoothly through the two-phase region below T_c, and fits the values of many important universal amplitude ratios.

However, both numerical and analytical [17] calculations lead to the prediction of a small but unphysical cusp in the variation of the surface tension $\Sigma(T,h)$ on crossing the critical isotherm at positive h, i.e., on entering the γ region of the phase diagram: see Fig. 1(a). This unanticipated behavior represents a shortcoming of the EdGF theory that is found to originate in the predicted variation of the order parameter profile, $M(z)$, in the immediate vicinity of $T=T_c$ when it passes through the critical value $M(z_0)=0$. An improved local functional theory might avoid this difficulty. To that end, it may be worthwhile to investigate the generalized or GdGF theory [6]. However, the undesirable feature may still remain since we are inclined to believe that the origin of the cusp is associated rather directly with the single, scalar order-parameter formulation: both EdGF and GdGF theories employ a simple scalar order parameter which cannot avoid "local criticality" when the interfacial profile crosses from one phase to another at $T=T_c$. In response to this observation, Mikheev and Fisher [48] have addressed the formulation of two-order-parameter theories in which, in particular, the local energy fluctuation, as a second "critical density," plays a role; but a practicable scheme of approximation has not so far been achieved.

Nevertheless, the application of EdGF theory to other properties of fluid interfaces and surfaces, seems worthwhile (e.g., [13]) and in the present case the cusp in $s(\theta)$, the scaling function for the surface tension, produces a deviation of only a few percent from the naturally interpolated analytic variation. Accordingly, for numerical purposes we have adopted a smoothing procedure that removes the cusp; this yields the ameliorated angular function $\overline{s}(\theta)$ that is recorded numerically in Table I.

On this basis the universal scaling functions $S_\pm(\tilde{h})$ and $S_M^\pm(\tilde{m})$ have been calculated: see Figs. 4 and 5 which reveal significant features of the anticipated variation of the surface tension $\Sigma(T,h)$. In particular, the role of the analytic background contribution $\Sigma_0(T,h)$ can be assessed. Together with the improved theoretical predictions (6.8) for the universal surface tension amplitude ratios, P and Q, these results will be used elsewhere [22] to reanalyze the experimental data of Nagarajan, Webb, and Widom [14] and to compare with other experiments [18–20].

ACKNOWLEDGMENTS

The interest of B. Widom and P. J. Upton has been appreciated and we are indebted to H. W. Diehl, S. Dietrich, J. Indekeu, and B. Widom for helpful comments on a draft manuscript. The authors are grateful for the support of the National Science Foundation through grants CHE 99-81772 and CHE 03-01101.

[1] J. S. Rowlinson and B. Widom, *Molecular Theory of Capillarity* (Oxford University Press, London, 1982).
[2] M. E. Fisher and M. C. Barbosa, Phys. Rev. B **43**, 11177 (1991).
[3] H. W. Diehl and M. Smock, Physica A **281**, 268 (2000).
[4] H. W. Diehl and M. Smock, Eur. Phys. J. B **21**, 567 (2001).
[5] M. E. Fisher and P. J. Upton, Phys. Rev. Lett. **65**, 2402 (1990).
[6] M. E. Fisher and P. J. Upton, Phys. Rev. Lett. **65**, 3405 (1990).
[7] N. B. Wilding, Phys. Rev. Lett. **78**, 1488 (1997).
[8] M. E. Fisher and S.-Y. Zinn, J. Phys. A **31**, L629 (1998).
[9] M. E. Fisher, S.-Y. Zinn, and P. J. Upton, Phys. Rev. B **59**, 14533 (1999). Note the erratum [**64**, 149901(E) (2001)] stating that the third line of Eq. (5.16), for the expansion coefficient d_1 of $n(\theta)$, lacks a factor b^2: it should read: $-\frac{1}{2}\left[\left(\frac{1}{4}-\beta\right)q^2+\left(3\beta-\frac{1}{2}\right)b^2\right]l_2q^2$.
[10] F. Ramos-Gómez and B. Widom, Physica A **104**, 595 (1980).
[11] J. W. Cahn and J. E. Hilliard, J. Chem. Phys. **28**, 258 (1958).
[12] B. Widom, J. Chem. Phys. **67**, 872 (1977).
[13] Z. Borjan and P. J. Upton, Phys. Rev. E **63**, 065102 (2001).
[14] N. Nagarajan, W. W. Webb, and B. Widom, J. Chem. Phys. **77**, 5771 (1982).
[15] R. G. Howland, N.-C. Wang, and C. M. Knobler, J. Chem. Phys. **73**, 522 (1980).
[16] S. Greer, Phys. Rev. A **14**, 1770 (1976).

[17] S.-Y. Zinn, Ph.D. thesis, University of Maryland, 1997.
[18] I. L. Pegg, M. C. Goh, R. L. Scott, and C. M. Knobler, Phys. Rev. Lett. **55**, 2320 (1985).
[19] M. Amara, M. Privat, R. Bennes, and E. Tronel-Peyroz, Europhys. Lett. **16**, 153 (1991).
[20] T. Mainzer-Althof and D. Woermann, Physica A **234**, 623 (1997).
[21] J. Ataiyan and D. Woermann, Pure Appl. Chem. **67**, 889 (1995).
[22] S.-Y. Zinn and M. E. Fisher (unpublished).
[23] H. B. Callen, *Thermodynamics* (Wiley, New York, 1960).
[24] B. Widom, in *Phase Transitions and Critical Phenomena*, edited by C. Domb and M. S. Green (Academic, London, 1972), Vol. 2, p. 72.
[25] H. T. Davis, *Statistical Mechanics of Phases, Interfaces, and Thin Films* (VCH, New York, 1996).
[26] J. W. Cahn, J. Chem. Phys. **66**, 3667 (1977).
[27] It is worth pointing out that modifying the prefactor J_0 in (2.8) by allowing it to embody, say, a singular T-dependence in an attempt to accommodate a value $\eta \neq 0$ [as one might interpret the sense of remarks by S. Fisk and B. Widom, J. Chem. Phys. **50**, 3219 (1969), or of Ref. [1] in Eqs. (9.32) and (9.48)] cannot actually yield a well defined critical-point correlation function with $\eta \neq 0$, i.e., with a decay of the form $1/r^{d-2+\eta}$ which serves to define η. Other attempts by specifically introducing nonlinear terms into the postulated critical-point differential equation for the correlation function have been analyzed by D. J. Klinger, M. E. Fisher, and S. Fishman, J. Chem. Phys. **80**, 3392 (1984), and shown to be unacceptable when $\eta \neq 0$ since the hyperscaling relation $2-\eta = d(\delta-1)/(\delta+1)$ (valid for $d \leqslant 4$) is violated. It is, of course, such difficulties that motivate the Fisher-Upton theory expounded in Sec. III.
[28] H. Nakanishi and M. E. Fisher, Phys. Rev. Lett. **49**, 1565 (1982).
[29] M. E. Fisher and P.-G. de Gennes, C. R. Seances Acad. Sci., Ser. B **287**, 207 (1978).
[30] G. Floeter and S. Dietrich, Z. Phys. B: Condens. Matter **97**, 213 (1995).
[31] E. Eisenriegler, M. Krech, and S. Dietrich, Phys. Rev. Lett. **70**, 619 (1993).
[32] M. Krech, E. Eisenriegler, and S. Dietrich, Phys. Rev. E **52**, 1345 (1995).
[33] E. Eisenriegler, M. Krech, and S. Dietrich, Phys. Rev. B **53**, 14377 (1996).
[34] M. E. Fisher and H. Au-Yang, Physica A **101**, 255 (1980).
[35] P. J. Upton, Phys. Rev. B **45**, 8100 (1992).
[36] E. Brézin, D. J. Wallace, and K. G. Wilson, Phys. Rev. Lett. **29**, 591 (1971).
[37] E. Brézin, D. J. Wallace, and K. G. Wilson, Phys. Rev. B **7**, 232 (1973).
[38] It should also be noted that M, h, $A_s(M,T)$, $\xi^2/2\chi$, etc., now carry dimensions (in contrast to the formulation in Ref. [9]) so that the corresponding angular functions $m(\theta)$, $l(\theta)$, $n(\theta)$, $a_\infty(\theta)$, etc., have appropriate dimensions. Consequently, l_0, m_0, and $a_{\infty,0} \equiv a_\infty(0)$, etc., also gain dimensions. However, the angular function $k(\theta)$ for the reduced temperature is kept dimensionless as are the parametric variables r and θ.
[39] One may [following P. J. Upton (private communication)] conveniently use angular functions $n_\pm(\theta)$ for the auxiliary free energy $W(M;T,h_\infty)$ when $h_\infty = 0$. These are related to $k(\theta)$ and $n(\theta)$ via $n_+(\theta) = n(\theta) - [k(\theta)/k(0)]^{2-\alpha} n(0)$ when $t > 0$ and $n_-(\theta) = n(\theta) - [k(\theta)/k(-\theta_1)]^{2-\alpha} n(\theta_1)$ when $t < 0$. Then the function $w(\theta;\theta_\infty)$ in (4.11) reduces to $n_+(\theta)$ when $\theta_\infty = 0$ ($h = 0, t > 0$) and to $n_-(\theta)$ when $\theta_\infty = \pm\theta_1$ ($h = 0, t < 0$).
[40] K. Binder, in *Phase Transitions and Critical Phenomena*, edited by C. Domb and M. S. Green (Academic, New York, 1983), Vol. 8, p. 1.
[41] H. W. Diehl, in *Phase Transitions and Critical Phenomena*, edited by C. Domb and J. L. Lebowitz (Academic, London, 1986), Vol. 10, p. 75.
[42] H. W. Diehl, Int. J. Mod. Phys. B **11**, 3503 (1997).
[43] W. H. Press, S. A. Teukolsky, W. T. Vetterling, and B. P. Flannery, *Numerical Recipes*, 2nd ed. (Cambridge University Press, New York, 1992), Sec. 4.4.
[44] M. Campostrini, A. Pelissetto, P. Rossi, and E. Vicari, Phys. Rev. E **65**, 066127 (2002).
[45] P. Butera and M. Comi, Phys. Rev. B **62**, 14837 (2000).
[46] J. Engels, L. Fromme, and M. Seniuch, Nucl. Phys. B **655**, 277 (2003).
[47] R. F. Kayser and H. J. Raveché, Phys. Rev. A **29**, 1013 (1984).
[48] L. V. Mikheev and M. E. Fisher, J. Stat. Phys. **66**, 1225 (1992); J. Low Temp. Phys. **90**, 119 (1993); Phys. Rev. Lett. **70**, 186 (1993); Phys. Rev. B **49**, 378 (1994).
[49] *Phase Transitions and Critical Phenomena*, Vol. 10, edited by C. Domb and J. L. Lebowitz (Academic, New York, 1986).